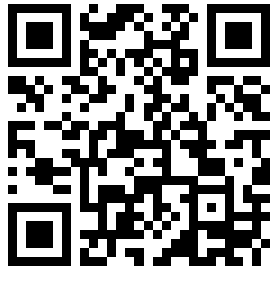

BNWL-1002
(ENDF-127)
UC-80

ETOX, A CODE TO CALCULATE GROUP CONSTANTS FOR NUCLEAR REACTOR CALCULATIONS

May 1969

AEC RESEARCH & DEVELOPMENT REPORT

BNWL-1002

BATTELLE NORTHWEST
BATTELLE MEMORIAL INSTITUTE
PACIFIC NORTHWEST LABORATORY
BATTELLE BOULEVARD, P. O. BOX 999, RICHLAND, WASHINGTON 99352

LEGAL NOTICE

PACIFIC NORTHWEST LABORATORY
RICHLAND, WASHINGTON
operated by
BATTELLE MEMORIAL INSTITUTE
for the
UNITED STATES ATOMIC ENERGY COMMISSION UNDER CONTRACT AT(45-1)-1830

AEC-RL RICHLAND, WASH.

BNWL-1002
(ENDF-127)
UC-80, Physics

ETOX, A CODE TO CALCULATE GROUP CONSTANTS FOR NUCLEAR REACTOR CALCULATIONS

By

R. E. Schenter
J. L. Baker
Physics Research Department
Physics and Engineering Division

and

R. B. Kidman
Reactor Physics and Operations Department
FFTF Division

May 1969

BATTELLE MEMORIAL INSTITUTE
PACIFIC NORTHWEST LABORATORY
RICHLAND, WASHINGTON 99352

Printed in the United States of America
Available from
Clearinghouse for Federal Scientific and Technical Information
National Bureau of Standards, U.S. Department of Commerce
Springfield, Virginia 22151
Price: Printed Copy $3.00; Microfiche $0.65

ETOX, A CODE TO CALCULATE GROUP CONSTANTS FOR NUCLEAR REACTOR CALCULATIONS

R. E. Schenter, J. L. Baker, and R. B. Kidman

ABSTRACT

Computer code ETOX (ENDF/B TO 1DX) calculates group constants for reactor calculations from currently available nuclear data. The code is specifically designed to use the Evaluated Nuclear Data File (ENDF/B) as input for microscopic cross section values. Output from this code includes punched cards in the Bondarenko format which can be used as input to the fast reactor codes FCC-IV and 1DX. Running time on a UNIVAC 1108 computer ranges from 13 to 600 sec per isotope. The current version of ETOX is restricted to a maximum of 99 energy groups.

TABLE OF CONTENTS

ETOX, A CODE TO CALCULATE GROUP CONSTANTS FOR NUCLEAR REACTOR CALCULATIONS

R. E. Schenter, J. L. Baker, and R. B. Kidman

I. INTRODUCTION

Fast reactor calculations[1] have been successfully performed using the multigroup method of Bondarenko et al.[2] One of the principal advantages of this method is that calculations can be made for reactors of various compositions using the same set of multigroup constants. Consequently, there has arisen a need to calculate these multigroup constants from more recent and presumably more accurate basic nuclear data. This report describes the computer code ETOX which calculates these constants using as input the basic nuclear data contained in the Evaluated Nuclear Data File (ENDF/B).[3] Output from this code includes "infinitely dilute" group cross sections, inelastic transfer matrices, and temperature dependent self-shielding factors for arbitrary values of σ_o (total cross section per atom). The output is given on punched cards in a format consistent for input to the fast reactor codes FCC-IV[4] and 1DX.[5]

II. GROUP CONSTANTS - DEFINITIONS

In the multigroup constant scheme, the microscopic group average cross section values for the "Ith" group and "jth" isotope are given by the following equation:

$$\bar{\sigma}^{I}_{x_j} = \int^{I} \sigma_{x_j}(E,T)\phi(E)dE \Big/ \int^{I} \phi(E)dE, \qquad (2.1)$$

where $\sigma_{x_j}(E,T)$ represents a particular energy and temperature dependent cross section. The subscript x represents either

capture, elastic, inelastic, or fission.† Following Bondarenko,[2] the neutron flux, $\phi(E)$, is assumed to vary as

$$\phi(E) = \phi_o(E) \Big/ \Sigma_t(E), \tag{2.2}$$

where $\Sigma_t(E)$ is the total macroscopic cross section of the medium. $\phi_o(E)$ is assumed to follow a Fermi spectrum except for the high energy groups dominated by the fission spectrum. That is,

$$\begin{aligned} \phi_o(E) &= \text{Constant} \times E^{-1} \text{ for } 0 \leq E \leq EF \\ &= \text{Constant} \times \sqrt{E} \times e^{(-E/CFF)} \text{ for } E > EF, \end{aligned} \tag{2.3}$$

where the constants EF and CFF are determined by the fission spectrum of the principal fissile isotope. This definition of $\phi(E)$ allows for flux depression in the resonance region.

Equation (2.1) implies a very time consuming method of calculating the group average cross section for every different temperature or reactor composition. The introduction of a set of basic cross sections to be multiplied by appropriate correction factors has proven to be more convenient;

$$\bar{\sigma}^I_{x_j} = f^I_{x_j} \langle \sigma_{x_j} \rangle^I, \tag{2.4}$$

where the bracket of a function is defined as an average with respect to the standard spectrum $\phi_o(E)$

$$\langle g \rangle^I = \int^I g(E,T)\phi_o(E)dE \Big/ \int^I \phi_o(E)dE. \tag{2.5}$$

---

† *Equation (2.1) does not represent the appropriate averaging of the total cross section in the multigroup scheme due to its inverse appearance in the neutron balance equations. See Appendix A and Bondarenko[2] for a further discussion of this point.*

The quantity $\langle\sigma_{x_j}\rangle^I$, called the "infinitely dilute cross section," is reactor and temperature independent.† The correction factor $f^I_{x_j}$, the "resonance self-shielding factor," contains composition and temperature information and is defined by Equation (2.4) since Equation (2.1) and (2.5) define $\bar{\sigma}^I_{x_j}$ and $\langle\sigma_{x_j}\rangle^I$, respectively. The shielding factor $f^I_{x_j}$ can be expressed (See Appendix A) as a function of temperature and $\sigma^I_{o_j}$ (total cross section per atom). The variables $\sigma^I_{o_j}$ and T are input parameters to the ETOX code. The parameter $\sigma^I_{o_j}$ represents the total macroscopic cross section due to all atoms (except the jth atoms) divided by the atomic density of the jth atoms. In the Bondarenko scheme it is assumed to be constant in energy over the group integrations. Its value is calculated by iterative procedures in the codes which use the output of ETOX.

The shielding factors $f^I_{x_j}$ are expressed in terms of "bracketed" functions as

$$f^I_{x_j}(T,\sigma^I_{o_j}) = \frac{1}{\langle\sigma_{x_j}\rangle^I} \left\langle \frac{\sigma_{x_j}}{\sigma_{t_j} + \sigma^I_{o_j}} \right\rangle^I \Bigg/\!\Bigg/ \left\langle \frac{1}{\sigma_{t_j} + \sigma^I_{o_j}} \right\rangle^I , \qquad (2.6)$$

where σ_{t_j} is the total energy and temperature dependent microscopic cross section of isotope j.

The shielding factors and infinitely dilute cross sections constitute the bulk of group constants needed in a multigroup reactor calculation. The remaining group constants are also expressed in terms of "bracketed" functions. Consequently, the main function of computer code ETOX is to read in the microscopic cross section data and then use this data to

† *Infinitely dilute cross sections are not strictly temperature independent. However, calculations indicate that their variation with temperature is extremely small.*

calculate integrals of the type given in Equation (2.5). The code does this for arbitrary sets of values of medium temperature and $\sigma_{o_j}^{I}$. From the resulting sets of group constants, a particular set appropriate to a given reactor may be constructed using interpolation schemes such as those described in the code FCC-IV.[4]

The following list gives the specific group constants calculated by the code ETOX. Specific reference to a particular group or isotope will be omitted. In that case, $\langle\sigma_{t_j}\rangle^{I} \rightarrow \langle\sigma_t\rangle$ for the Ith group and the jth isotope.

$\langle\sigma_t\rangle$ = infinitely dilute total cross section ($\langle\sigma_t\rangle = \langle\sigma_c\rangle + \langle\sigma_e\rangle + \langle\sigma_{in}\rangle$),
$\langle\sigma_f\rangle$ = infinitely dilute fission cross section,
$\langle\sigma_c\rangle$ = infinitely dilute capture cross section,
$\langle\sigma_e\rangle$ = infinitely dilute elastic cross section,
$\langle\sigma_{in}\rangle$ = infinitely dilute total inelastic scattering cross section [includes (n,2n) reaction],
$\langle\nu\rangle$ = average number of neutrons released per fission,
$\langle\mu_e\rangle$ = average cosine of the elastic scattering angle,
$\langle\xi\rangle$ = average lethargy change by elastic scattering,
$\sigma_{d,e}$ = elastic slowing-down cross section,
$f_t(\sigma_o,T)$ = total cross section self-shielding factor,
$f_e(\sigma_o,T)$ = elastic cross section self-shielding factor,
$f_f(\sigma_o,T)$ = fission cross section self-shielding factor,
$f_c(\sigma_o,T)$ = capture cross section self-shielding factor,
$\overline{\sigma_{in}^{(I\rightarrow k)}}$ = inelastic transfer cross section from group I to group k [includes (n,2n) reaction].

Definitions of the above quantities follow from Equations (2.5) and (2.6) except for the following:

$$\sigma_{d,e} = \langle\xi\rangle \langle\sigma_e\rangle / \Delta u \quad (\Delta u \text{ - lethargy interval of the group}), \tag{2.7}$$

$$f_t(\sigma_o,T)^{\dagger} = \frac{1}{\langle\sigma_t\rangle}\left[\left(\frac{1}{\sigma_t + \sigma_o}\Big/\frac{1}{(\sigma_t + \sigma_o)^2}\right) - \sigma_o\right] \qquad (2.8)$$

and

σ_{in} (I→k), which is described in Section V.

III. OUTLINE OF CODE LOGIC

The function of the ETOX code is to calculate the group constants defined in Section II using the ENDF/B[††] data tape as input. The steps below indicate the procedure followed by the code:

1) Read input data and first three files of ENDF/B.
2) Calculate cross sections at fine-group intervals from point data given in File 3 using the interpolation methods specified by ENDF/B.
3) Calculate group constants in the non-resonance region using the cross sections at the fine-group intervals.
4) Calculate group constants in the resonance region using the resonance parameters given in File 2.
5) Read File 5 and calculate inelastic scattering matrices.
6) Punch and write group constants in the 1DX[(4)] or FCC-IV[(5)] formats.

The steps specified above are illustrated in Figure 1 with a schematic diagram of the code, where the names of the major subroutines used are also shown. Appendix D gives a brief description of all the subroutines in ETOX. The fine-group intervals mentioned in Step 2 are calculated to be of equal lethargy size within a group. Their number, NFG(I) for the Ith group, is determined by finding the largest of the following:

---

† *See Appendix A.*

†† *In this report the term ENDF/B will represent both the Evaluated Nuclear Data File and its associated "specification" document (Reference 3).*

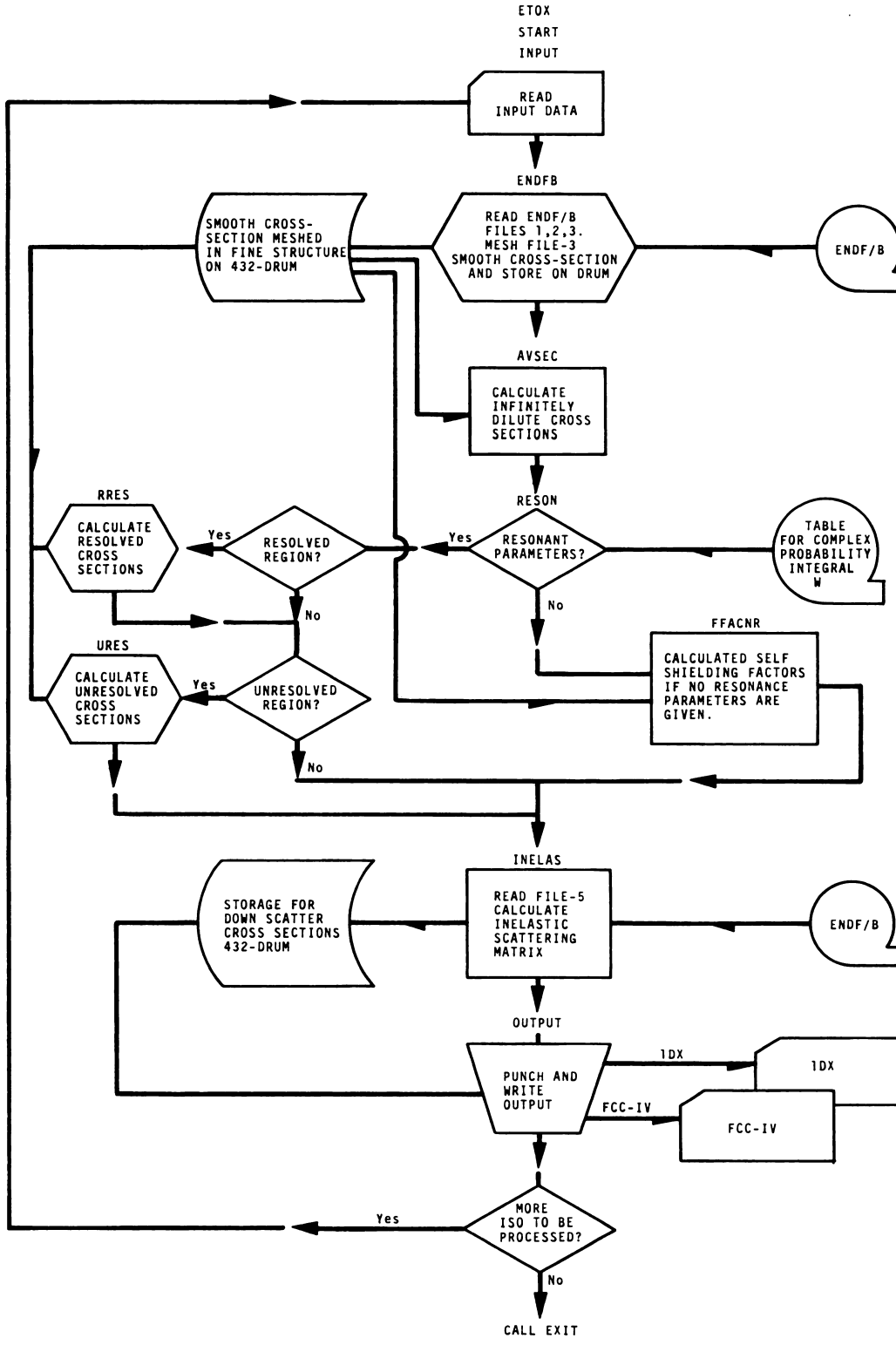

FIGURE 1. Schematic Diagram of ETOX

A. The closest integer found from the division of the lethargy size of the group by a given input lethargy interval (DELMAX).†

B. The product of the number of total cross section points in the group, as determined from File 3, times a given input parameter (NFMPD/4).†

The energy bounds of the various group structures (group, fine group, ultrafine group) and regions (resolved, unresolved, self-shielding, etc.) are diagramed in Appendix E for a typical isotope.

IV. RESONANCE CALCULATIONS

Resonance calculations, both resolved and unresolved, are based on the prescription given in ENDF/B, where partial cross sections are given in terms of sums of Doppler broadened single-level Breit-Wigner functions with additional "floor" corrections†† to allow for deviations of the cross section from the Breit-Wigner formulas. The following expressions give the formulas for these cross sections for a temperature T and energy E in the laboratory system:

$$\sigma_f(E,T) = \sum_{s=1}^{N} \sum_{r=1}^{N_s} \sigma_f^s(E,T)_r + \sigma_{f_F}(E), \qquad (4.1)$$

$$\sigma_c(E,T) = \sum_{s=1}^{N} \sum_{r=1}^{N_s} \sigma_c^s(E,T)_r + \sigma_{c_F}(E), \qquad (4.2)$$

---

† *The quantities DELMAX and NFMPD are secondary type input parameters. The distinction between the two types of input parameters, primary and secondary, is discussed in Appendix G.*

†† *Cross sections obtained from ENDF/B file 3.*

$$\sigma_c(E,T) = \sum_{s=1}^{N} \sum_{r=1}^{N_s} \sigma_e^s(E,T)_r + \sigma_p(E) + \sigma_{e_F}(E), \tag{4.3}$$

$$\sigma_t(E,T) = \sigma_f(E,T) + \sigma_c(E,T) + \sigma_e(E,T), \tag{4.4}$$

where s represents a particular sequence of resonances, s = (ℓ,j), and r the resonances belonging to that sequence, ℓ = orbital and j = total angular momentum quantum numbers,†

$$\sigma_{x_F}(E) = \text{"floor" correction} \quad (x = f,c,e), \tag{4.5}$$

$$\sigma_x^s(E,T)_r = \sigma_{o_r}^s(E) \frac{\Gamma_{xr}^s}{\Gamma_r^s(E)} \psi\left(\xi_r^s, X_r^s\right) \quad (x = f,c), \tag{4.6}$$

$$\sigma_e^s(E,T)_r = \sigma_{o_r}^s(E) \left[\Gamma_e^s(E)\, \psi\left(\xi_r^s, X_r^s\right) + \varphi_\ell(E)\, \chi\left(\xi_r^s, X_r^s\right)\right], \tag{4.7}$$

$$\sigma_p(E) = \frac{4\pi}{K^2} \sum_{\ell} (2\ell + 1) \sin^2 \varphi_\ell(E), \tag{4.8}$$

$$\xi_r^s(E,T) = \Gamma_r^s(E) \Big/ \Delta(T), \tag{4.9}$$

$$X_r^s(E) = \left(E - E_r^s\right) \Big/ \Gamma_r^s(E). \tag{4.10}$$

RESOLVED RESONANCES

For the resolved resonance calculations the energy region is divided into ultrafine groups where generally these group boundaries are determined to be a half width on either side of a resolved resonance energy (see Figure 2).

† *More detailed and complete definitions of the terms in Equations (4.1) through (4.10) are given in Appendix B.*

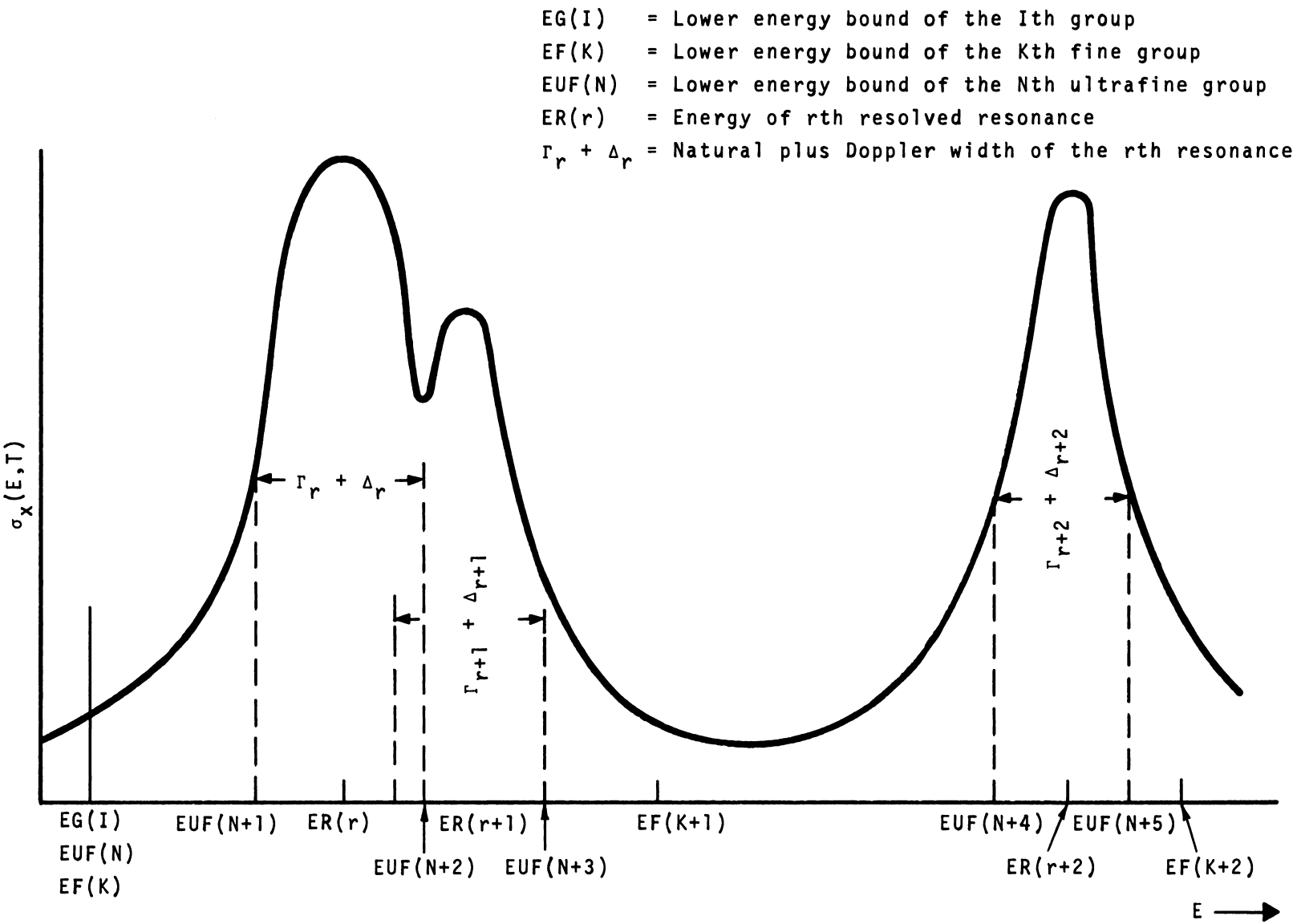

FIGURE 2. Typical Group Structures in the Resolved Resonance Region.

In this region cross section integrals are calculated for each ultrafine group using the Romberg integration method.[7] The ultrafine structure takes advantage of the Romberg technique giving a very good speed-accuracy factor since in general the second derivatives of the cross section will be constant in sign. This leads to a minimum number of integration points needed to be evaluated to obtain convergence.†

For each ultrafine group N within group I, the following integrals are calculated:††

$$\bar{\sigma}_x^{I,N} \equiv \int_{EUF(N)}^{EUF(N+1)} \frac{\sigma_x(E,T)dE}{[\sigma_t(E,T) + \sigma_o]E} \qquad (x = f,c,e), \tag{4.11}$$

$$W^{I,N} \equiv \int_{EUF(N)}^{EUF(N+1)} \frac{dE}{[\sigma_t(E,T) + \sigma_o]E}, \tag{4.12}$$

$$WT^{I,N} \equiv \int_{EUF(N)}^{EUF(N+1)} \frac{dE}{[\sigma_t(E,T) + \sigma_o]^2 E}, \tag{4.13}$$

$$\langle \sigma_x \rangle^{I,N} \equiv \int_{EUF(N)}^{EUF(N+1)} \frac{\sigma_x(E,T)dE}{E} \qquad (x = f,c,e). \tag{4.14}$$

† *The code uses a Romberg integration order of 7. If no convergence is obtained after seven cycles an error message is written.*

†† *The standard spectrum is assumed to vary as I/E for all resonance calculations.*

In the above integrals the "floor" correction cross sections are assumed to be constant with values given as

$$\bar{\sigma}_{x_F}^{N} = 1/2 \left\{ \sigma_{x_F}\left[EUF(N)\right] + \sigma_{x_F}\left[EUF(N+1)\right] \right\}. \qquad (4.15)$$

Group infinitely dilute cross sections and self-shielding factors are given in terms of sums of the integrals in Equations (4.11) through (4.14) as

$$\langle \sigma_x \rangle^{I} = \sum_{N=1}^{N_I} \langle \sigma_x \rangle^{I,N} \Big/ ln\left[EG(I+1)/EG(I)\right], \qquad (4.16)$$

$$f_x^I = \frac{1}{\langle \sigma_x \rangle^{I}} \frac{\sum_{N=1}^{N_I} \bar{\sigma}_x^{I,N}}{\sum_{N=1}^{N_I} W^{I,N}}, \qquad (4.17)$$

$$f_t^I = \frac{1}{\langle \sigma_x \rangle^{I}} \left[\frac{\sum_{N=1}^{N_I} W^{I,N}}{\sum_{N=1}^{N_I} WT^{I,N}} - \sigma_o \right], \qquad (4.18)$$

where N_I is the number of ultrafine groups in the Ith group.

An important factor in obtaining an optimum speed-accuracy factor for the resolved resonance region is to include in the calculation only those resonances which contribute significantly in a given ultrafine group. This is accomplished in the code by testing a given resonance to see if it is within

a certain fixed multiple† of its total width from the given ultrafine group. The testing process works outward both to lower and higher energies from the given ultrafine group. When three resonances on each side of the ultrafine group do not pass the test, the process is terminated.

UNRESOLVED RESONANCES

Unresolved calculations follow closely the methods and approximations used in the MC^2 code,[6] where infinitely dilute and self-shielded cross sections are calculated at discrete energy points E* in the unresolved energy region. Group cross sections are obtained by averaging values calculated at equal lethargy spaced points in the group.††

The infinitely dilute and self-shielded cross sections are given as

$$\left\langle \sigma_x(E^*) \right\rangle = \frac{\int_{E_1}^{E_2} \frac{\sigma_x(E,T)\,dE}{E}}{\int_{E_1}^{E_2} \frac{dE}{E}} \qquad (x = f,c,e), \qquad (4.19)$$

† *The fixed multiple (NTOL) is a secondary input parameter in the code where its initial value has been set to be 5.*

†† *The lethargy spacing, DELUMX, is a secondary input parameter.*

$$\overline{\sigma_x(E^*)} = \frac{\int_{E_1}^{E_2} \frac{\sigma_x(E,T)dE}{[\sigma_t(E,T) + \sigma_o]E}}{\int_{E_1}^{E_2} \frac{dE}{[\sigma_t(E,T) + \sigma_o]E}}, \tag{4.20}$$

and

$$\overline{\sigma_t(E^*)} = \frac{\int_{E_1}^{E_2} \frac{dE}{[\sigma_t(E,T) + \sigma_o]E}}{\int_{E_1}^{E_2} \frac{dE}{[\sigma_t(E,T) + \sigma_o]^2 E}} - \sigma_o, \tag{4.21}$$

where E^* is some energy point in the energy range (E_1, E_2) which is assumed to contain many narrow resonances. Equations (4.19) through (4.21) are simplified if one assumes that the energy variation in the integrands in the above integrals only occurs in the rapidly varying resonance parts of the ψ function. The slowly varying terms are evaluated at the energy E^*. In this approximation the elastic cross section, for example, is written as†

† *As in MC² (Reference 6) the interference-scattering term in the elastic cross section is ignored.*

$$\sigma_e(E,E^*,T) = \sum_{s=1}^{N} \sum_{r=1}^{N_s} \frac{6\, {}^s_{o_r}(E^*)\Gamma^s_{e_r}(E^*)}{\Gamma^s_r(E^*)} \psi\left[\xi^s_r(E^*),\ 2(E - E^s_r)/\Gamma^s_r(E^*)\right]$$

$$+ \sigma_p(E^*) + \sigma_{e_F}(E^*) \qquad (4.22)$$

The above assumption should be a good approximation since in the unresolved region the energy interval $(E_2 - E_1)$ may be picked to be small with respect to variations in the slowly varying components of the cross section. With this approximation Equations (4.19) through (4.21) become†

$$\left\langle \sigma_x(E^*) \right\rangle = \frac{1}{E_2 - E_1} \int_{E_1}^{E_2} \sum_s \sum_r \sigma^s_{x_r}(E,E^*)dE + \sigma_{x_F}(E^*) + \sigma_p(E^*)\delta_{x_e}, \qquad (4.23)$$

$$\overline{\sigma_x(E^*)} = \left[\int_{E_1}^{E_2} \frac{\sum_s \sum_r \sigma^s_{x_r}(E,E^*)de}{\left(\sum_s \sum_r \sigma^s_{t_r}(E,E^*) + \bar{\sigma}_p \right)} \Bigg/ \right.$$

$$\left. \int_{E_1}^{E_2} \frac{dE}{\left(\sum_s \sum_r \sigma^s_{t_r}(E,E^*) + \bar{\sigma}_p \right)} \right] + \sigma_{x_F}(E^*) + \sigma_p(E^*)\delta_{x_e}, \qquad (4.24)$$

† *Temperature dependence will not be explicitly indicated in the remaining Equations of this section. The symbol* δ_{x_e} *is o when* $x \neq e$ *and 1 when* $x = e$.

$$\overline{\sigma_t(E^*)} = \left[\int_{E_1}^{E_2} \frac{dE}{\left(\sum_s \sum_r \sigma_{t_r}^s(E,E^*) + \bar{\sigma}_p\right)} \Bigg/ \int_{E_1}^{E_2} \frac{dE}{\left(\sum_s \sum_r \sigma_{t_r}^s(E,E^*) + \bar{\sigma}_p\right)^2}\right] - \sigma_o, \tag{4.25}$$

where

$$\bar{\sigma}_p = \sigma_p(E^*) + \sigma_{f_F}(E^*) + \sigma_{c_F}(E^*) + \sigma_{e_F}(E^*) + \sigma_o. \tag{4.26}$$

With the assumption of many resonances in the interval $(E_2 - E_1)$, the resonance contributions in the above integrals are treated statistically. The interval $(E_2 - E_1)$ is replaced by the average spacing of the resonances of sequence s, D^s, times the number N^s contained in the interval. The summation over resonances in a given sequence is then replaced with a double integration over a Porter-Thomas (chi-squared) distribution with n and m degrees of freedom. Symbolically

$$\frac{1}{N^s} \sum_r f_r^s \rightarrow \int_o^\infty \int_o^\infty P_{n^s}(y) P_{m^s}(z) f^s(y,z)\,dy\,dz \equiv \left\langle f^s \right\rangle_p^\dagger, \tag{4.27}$$

where

$$P_n(y) = \frac{n}{2} \frac{1}{\Gamma\left(\frac{n}{2}\right)} \left(\frac{ny}{2}\right)^{\frac{n}{2}-1} \exp\left(-\frac{ny}{2}\right). \tag{4.28}$$

---

† *In the ETOX code the statistical brackets are evaluated by the standard double summation techniques as described in Reference 3. (See Appendix E for the exact details.)*

Following the specifications of ENDF/B,[3] the functions $P_n(y)$ and $P_m(z)$ in Equation (4.27) represent the elastic and fission width† distributions, where

$$\Gamma^s_{c_r}(E^*) \rightarrow \Gamma^s_e(E^*,y) = y\Gamma^s_e(E^*), \tag{4.29}$$

$$\Gamma^s_{f_r}(E^*) \rightarrow \Gamma^s_f(E^*,z) = z\Gamma^s_f(E^*). \tag{4.30}$$

With the above replacements and the narrow resonance approximation such that

$$\int_{E_1}^{E_2} f(E)dE \rightarrow \int_{-\infty}^{\infty} f(E)dE, \tag{4.31}$$

Equation (4.23) becomes

$$\langle\sigma_x(E^*)\rangle = \sum_s \frac{1}{D_s} \left\langle \Gamma^s_x(E^*)\, 6^s_o(E^*) \int_o^{\infty} \psi(\xi^s,X)dX \right\rangle_P$$

$$+ \sigma_{x_F}(E^*) + \sigma_p(E^*)\delta_{x_e}. \tag{4.32}$$

Since††

$$\int_o^{\infty} \psi(\xi^s,X)dX = \frac{\pi}{2}, \tag{4.33}$$

independent of the value of ξ^s, the infinite dilute cross section is finally given as

---

† *For isotopes which do not have appreciable fission widths in the unresolved energy region the double integral in Equation (4.27) reduces to a single integral.*

†† *See Appendix B.*

$$\left\langle \sigma_x(E^*) \right\rangle = \frac{\pi}{2} \sum_s \frac{1}{D_s} \left\langle 6\, {}^s_o(E^*) \Gamma^s_x(E^*) \right\rangle_p + \sigma_{x_F}(E^*) + \sigma_p(E^*) \delta_{x_e} . \tag{4.34}$$

Due to the appearance of the resonance terms in the denominator of the expressions in Equations (4.24) and (4.25), the self-shielded cross sections require additional approximations and analysis for their evaluation. Consistent with the narrow resonance approximation, it is assumed that overlap effects between different resonances of the same sequence and overlap between more than one sequence may be ignored. The numerator, for example, in Equation (4.24) then becomes[6,8]

$$\text{NUM} = \sum_s \sum_r \int_{E_1}^{E_2} \frac{\sigma^s_{x_r}(E,E^*)}{\left(\sigma^s_{t_r}(E,E^*) + \bar{\sigma}_p\right)} \left[1 - \sum_{s' \neq s} \sum_{r'} \frac{\sigma^{s'}_{t_{r'}}(E,E^*)}{\left(\sigma^{s'}_{t_{r'}}(E,E^*) + \bar{\sigma}_p\right)} \right] dE, \tag{4.35}$$

Rewriting Equation (4.35) in terms of the line-shape functions $\psi(\xi^s_r, X^s_r)$ gives

$$\text{NUM} = \sum_s \sum_r \frac{\Gamma^s_{x_r}(E^*)}{\Gamma^s_r(E^*)} \int_{E_1}^{E_2} \frac{\psi(\xi^s_r, X^s_r)}{\left(\psi(\xi^s_r, X^s_r) + \beta^s_r\right)} \left[1 - \sum_{s' \neq s} \sum_{r'} \frac{\psi(\xi^{s'}_{r'}, X^{s'}_{r'})}{\left(\psi(\xi^{s'}_{r'}, X^{s'}_{r'}) + \beta^{s'}_{r'}\right)} \right] dE, \tag{4.36}$$

where

$$\beta_r^s = \bar{\sigma}_p / 6\, {}^s o_r (E^*). \tag{4.37}$$

The sequences s' are uncorrelated with respect to s in Equation (4.36). Consequently, it is necessary to integrate the primed summations over the probability of finding resonance r' of s' at a separation δ from resonance r of s, where δ ranges from $-(E_r - E_1)$ to $(E_2 - E_r)$ and E_r is the location of the resonance r in the interval $E_2 - E_1$.† With this and the statistical analysis following Equation (4.25), Equation (4.36) is given as[6]

$$\mathrm{NUM} = (E_2 - E_1) \sum_s \frac{\left\langle \Gamma_x^s(E^*) J(\xi^s, \beta^s) \right\rangle_p}{D_s} \left[1 - \sum_{s' \neq s} \frac{\left\langle \Gamma^{s'}(E^*) J(\xi^{s'}, \beta^{s'}) \right\rangle_p}{D_{s'}} \right], \tag{4.38}$$

where the usual J integral is defined as

$$J(\xi^s, \beta^s) \equiv \int_0^\infty \frac{\psi(\xi^s, X)\, dX}{\left(\psi(\xi^s, X) + \beta^s\right)} . \tag{4.39}$$

The denominator in Equation (4.24) and the terms in Equation (4.25) are evaluated in a similar manner as that given above for the numerator in Equation (4.24). The final expressions for the self-shielded cross sections are

† *This sentence is almost a direct quote from that given in Reference 6.*

$$\overline{\sigma_x(E^*)} = \bar{\sigma}_p \sum_s a_x^s \left(1 - \sum_{s' \neq s} b^{s'}\right) \Big/ \left[1 - \sum_s b^s \left(1 - \sum_{s' \neq s} b^{s'}\right)\right]$$

$$+ \sigma_{x_F} + \sigma_p \delta x_e, \tag{4.40}$$

$$\overline{\sigma_t(E^*)} = \bar{\sigma}_p \left[1 - \sum_s b^s \left(1 - \sum_{s' \neq s} b^{s'}\right)\right] \Big/$$

$$\left[1 - \sum_s c^s \left(1 - \sum_{s' \neq s} c^{s'}\right)\right] - \sigma_o, \tag{4.41}$$

where†

$$a_x^s = \left\langle \Gamma_x^s J^s \right\rangle_P \Big/ D_s, \tag{4.42}$$

$$b^s = \left\langle \Gamma^s J^s \right\rangle_P \Big/ D_s, \tag{4.43}$$

$$c^s = \left\langle \Gamma^s K^s \right\rangle_P \Big/ D_s, \tag{4.44}$$

$$K^s = K(\xi^s, \beta^s) = \int_o^\infty \frac{\psi(\xi^s, X)[\psi(\xi^s, X) + 2\beta^s]}{[\psi(\xi^s, X) + \beta^s]^2} \, dX. \tag{4.45}$$

† *See Appendix G for the evaluations of the J and K integrals.*

V. INELASTIC SCATTERING

In general, the (n,n') and (n,2n) reactions of an isotope occur at energies above the isotope's resonance regions. Hence, when the (n,n') or (n,2n) group average cross sections are calculated, any departures from the standard spectrum, Equation (2.3), caused by the presence of resonances are neglected. An additional reason for doing this is that the fast reactor codes FCC-IV[4] and 1DX[5] are not programmed to accept self-shielding factors for inelastic scattering cross sections. When the definition of Equation (2.5) is used, the group average total and transfer cross sections are therefore calculated according to

$$\bar{\sigma}_x^i = \langle \sigma_x(E) \rangle^i \tag{5.1}$$

$$\overline{\sigma_x(i \to j)} = \langle \sigma_x(E) W_x(E \to j) \rangle^i, \tag{5.2}$$

where x refers to either the (n,n') or (n,2n) reaction; $\sigma_x(E)$ is the x reaction cross section obtainable from ENDF/B, File 3; and $W_x(E \to j)$ is the fraction of neutrons that scatter from an x reaction at energy E into group j. Since ETOX assumes upscatter cannot occur, j can only refer to group i or to groups lower in energy than group i.

Prior to evaluation of $W_x(E \to j)$, it is necessary to introduce the tabulated functions which ENDF/B provides for the description of the energy of inelastically scattered neutrons. If $P_x(E \to E')$ is the probability of inelastic scatter from E to E', then ENDF/B defines it as a sum over NK partial distributions,

$$P_x(E \to E') = \sum_{k=1}^{NK} G_x^k(E) F_x^k(E \to E'), \tag{5.3}$$

where $G_x^k(E)$ is the fraction of scattered neutrons whose energy is governed by the $F_x^k(E \to E')$ energy distribution. The $G_x^k(E)$ and $F_x^k(E \to E')$ are tabulated functions to be found in ENDF/B, File 5. Additional conditions are

$$\int_o^\infty F_x^k(E \to E')dE' = 1 \tag{5.4}$$

$$\sum_{k=1}^{NK} G_x^k(E) = 1 \ . \tag{5.5}$$

Now, it frequently occurs that for a collision at energy E

$$\int_o^E F_x^k(E \to E')dE' < 1 \tag{5.6}$$

which causes

$$\int_o^E P_x(E \to E')dE' < 1 \ . \tag{5.7}$$

This is contrary to the assumption that only downscatter can occur. Thus, the $W_x(E \to j)$ cannot be found by a simple integration of $P_x(E \to E')$ over the energies of group j. Rather, $W_x(E \to j)$ must be evaluated in the following manner,

$$W_x(E \to j) = \sum_{k=1}^{NK} G_x^k(E) \frac{\int^j F_x^k(E \to E')dE'}{\int_o^E F_x^k(E \to E')dE'} \ , \tag{5.8}$$

where $\int^j \ldots dE'$ indicates an integration over the energies of group j. Equation (5.8) has to be modified for the case when j = i (ingroup scattering),

$$W_x(E\to i) = \sum_{k=1}^{NK} G_x^k(E) \frac{\int_{EG(i)}^{E} F_x^k(E\to E')dE'}{\int_{o}^{E} F_x^k(E\to E')dE'} , \qquad (5.9)$$

where EG(i) is the lower energy of group i.

Equation (5.8) and (5.9) now assure that

$$\sum_{j\geq i}^{NG} W_x(E\to j) = 1, \qquad (5.10)$$

where NG is the number of groups.

Since FCC-IV[4] and 1DX[5] do not handle the (n,2n) reaction explicitly, ETOX incorporates the (n,2n) reaction into its final inelastic total, $\bar{\sigma}_{in}^{i}$, and transfer cross sections, $\overline{\sigma_{in}(i\to j)}$, in the following way,

$$\bar{\sigma}_{in}^{i} = \bar{\sigma}_{n,n'}^{i} + \bar{\sigma}_{n,2n}^{i} \qquad (5.11)$$

$$\overline{\sigma_{in}(i\to j)} = \overline{\sigma_{n,n}(i\to j)} + \overline{2\sigma_{n,2n}(i\to j)} . \qquad (5.12)$$

ETOX prints and punches only the $\bar{\sigma}_{in}^{i}$ and $\overline{\sigma_{in}(i\to j)}$.

The sum in Equations (5.8) or (5.9) is over those secondary energy distributions, $F_x^k(E\to E')$, that ENDF/B finds necessary to adequately describe the collision at energy E. Now, ENDF/B allows for ten different types of $F_x^k(E\to E')$, but the sum does not have to include all ten types, and a single type may be included several times. Below is a brief description of how the various types of $F_x^k(E\to E')$ are integrated to obtain the integrals in Equations (5.8) and (5.9):

Arbitrary Tabulated Function (LF = 1). The present version of ETOX does not handle this type.

Discrete Final Energy (LF = 2). If Θ is the final energy to which neutrons are scattered, the integrals are simply replaced by 1 or 0 depending on whether Θ lies within the integral's limits.

Discrete Energy Loss (LF = 3). If Θ is the energy which neutrons lose when scattered, the integrals are 1 or 0 depending on whether $(E - \Theta)$ lies within the integral's limits.

General Evaporation Spectrum (LF = 4,5). For this type, $F_x^k(E \to E') = F(E'/\Theta)$ and one is interested in integrals like the following

$$\int_A^B F(E'/\Theta)dE'.$$

However, ENDF/B tabulates F as a function of Y, where $Y = E'/\Theta$. With this change of variables, the integral becomes

$$\int_A^B F(E'/\Theta)dE' = \Theta\int_{A/\Theta}^{B/\Theta} F(Y)dY.$$

The integral on the right is numerically carried out by applying the trapezoidal rule with unequal subintervals as determined by the ENDF/B data points that lie between the integral's limits. The nuclear temperature Θ is a constant for type LF = 4, but for LF = 5, Θ is a function of energy.

Simple Fission Spectrum (LF = 6,7). The integrals over the fission spectrum are replaced by the following

$$\int_A^B \sqrt{\frac{4E'}{\pi\Theta^3}}\exp(-E'/\Theta)dE' = \frac{2}{\sqrt{\pi}}\left[\sqrt{\frac{A}{\Theta}}\exp\left(-\frac{A}{\Theta}\right) - \sqrt{\frac{B}{\Theta}}\exp\left(-\frac{B}{\Theta}\right)\right]$$

$$+ \mathrm{ERF}\sqrt{\frac{B}{\Theta}} - \mathrm{ERF}\sqrt{\frac{A}{\Theta}},$$

where θ is the nuclear temperature [θ = constant for LF = 6, and $\theta = \theta(E)$ for LF = 7].

Maxwellian Distribution (LF = 8,9). The integrals over the Maxwellian distribution are replaced by the following,

$$\int_A^B \frac{E'}{\theta^2} \exp(-E'/\theta)dE' = \frac{1}{\theta}\left[(A + \theta)\exp(-A/\theta) - (B + \theta)\exp(-B/\theta)\right],$$

where θ is the nuclear temperature [θ = constant for LF = 8, and $\theta = \theta(E)$ for LF = 9].

WATT Spectrum (LF = 10). The integrals over the Watt Spectrum are replaced by the following,

$$\int_A^B \left[\frac{4}{\pi a^3 b}\right]^{1/2} \exp\left(-\frac{ab}{4}\right) \exp\left(-\frac{E'}{a}\right) \sinh\sqrt{bE'}\, dE' =$$

$$[\pi ab]^{-1/2}\left\{\exp\left[-\left(\sqrt{\frac{B}{a}} + \sqrt{\frac{ab}{2}}\right)^2\right] + \exp\left[-\left(\sqrt{\frac{A}{a}} - \sqrt{\frac{ab}{2}}\right)^2\right]\right.$$

$$\left. - \exp\left[-\left(\sqrt{\frac{B}{a}} - \sqrt{\frac{ab}{2}}\right)^2\right] - \exp\left[-\left(\sqrt{\frac{A}{a}} + \sqrt{\frac{ab}{2}}\right)^2\right]\right\} + \frac{1}{2}\left\{\mathrm{ERF}\left(\sqrt{\frac{B}{a}} - \sqrt{\frac{ab}{2}}\right)\right.$$

$$\left. - \mathrm{ERF}\left(\sqrt{\frac{A}{a}} - \sqrt{\frac{ab}{2}}\right) + \mathrm{ERF}\left(\sqrt{\frac{B}{a}} + \sqrt{\frac{ab}{2}}\right) - \mathrm{ERF}\left(\sqrt{\frac{A}{a}} + \sqrt{\frac{ab}{2}}\right)\right\},$$

where a and b are constants provided by ENDF/B.

VI. TYPICAL RESULTS AND DISCUSSION

Tables 1 and 2 give typical results for the calculations of group constants for the isotope of ^{239}Pu (MAT=1051) and natural occurring Fe (MAT=1020). The energy group structure, temperature, and σ_o values are the same as those used by Bondarenko.[2]

We believe the approximations in this code are consistent with the uncertainties of present cross section data, the limitations of the ENDF/B format, and the approximations in the codes using group constants as input. Preliminary calculations have been made for 26 and 50 group sets coupling the ETOX and 1DX[5] codes for several fast reactor cores.[1] The results from these calculations show close agreement with those generated using the "many group" (~1000) MC^2 code.[6] Table 3 gives typical results of fundamental mode calculations for the fast reactor assembly ZEBRA 6A.

TABLE 1. Group Constants for Fast Reactor Calculations (Fe Natural)

Infinite Dilute Cross Sections

Energy /	Groups	σ_T	σ_F	ν	σ_C	σ_{inel}	σ_{el}	μ_e	ξ	$\sigma_{D(e)}$
6.5 - 10.5 MeV	1	3.606	.000	.00	.038	1.351	2.217	.820	.0060	.028
4.0 - 6.5 MeV	2	3.806	.000	.00	.004	1.388	2.414	.695	.0104	.052
2.5 - 4.0 MeV	3	3.376	.000	.00	.001	1.078	2.298	.481	.0182	.087
1.4 - 2.5 MeV	4	2.969	.000	.00	.001	.742	2.226	.264	.0259	.101
0.8 - 1.4 MeV	5	2.546	.000	.00	.003	.283	2.260	.231	.0271	.107
0.4 - 0.8 MeV	6	3.187	.000	.00	.005	.000	3.182	.149	.0297	.137
0.2 - 0.4 MeV	7	3.043	.000	.00	.005	.000	3.038	.091	.0321	.141
0.1 - 0.2 MeV	8	4.759	.000	.00	.005	.000	4.754	.084	.0323	.223
46.5 - 100 keV	9	5.012	.000	.00	.006	.000	5.006	.082	.0324	.211
21.5 - 46.5 keV	10	11.213	.000	.00	.025	.000	11.187	.080	.0325	.472
10.0 - 21.5 keV	11	3.822	.000	.00	.018	.000	3.804	.077	.0326	.161
4.65 - 10.0 keV	12	9.958	.000	.00	.050	.000	9.908	.075	.0327	.420
2.15 - 4.65 keV	13	5.763	.000	.00	.012	.000	5.751	.072	.0327	.244
1.0 - 2.15 keV	14	7.879	.000	.00	.098	.000	7.781	.070	.0328	.332
465 - 1000 eV	15	9.946	.000	.00	.017	.000	9.929	.068	.0329	.424
215 - 465 eV	16	11.015	.000	.00	.026	.000	10.988	.065	.0330	.471
100 - 215 eV	17	11.421	.000	.00	.034	.000	11.387	.063	.0331	.489
46.5 - 100 eV	18	11.424	.000	.00	.053	.000	11.371	.060	.0332	.490
21.5 - 46.5 eV	19	11.417	.000	.00	.073	.000	11.344	.058	.0332	.490
10.0 - 21.5 eV	20	11.376	.000	.00	.101	.000	11.275	.056	.0333	.488
4.65 - 10.0 eV	21	11.388	.000	.00	.149	.000	11.239	.053	.0334	.487
2.15 - 4.65 eV	22	11.498	.000	.00	.221	.000	11.277	.051	.0335	.490

Self-Shielding Factors

σ_o	f_c				f_t				f_e			
	10^3	10^2	10	0	10^3	10^2	10	0	10^3	10^2	10	0
2	1.000	.994	.987	.984	1.000	1.000	1.000	1.000	1.000	.998	.997	.997
3	1.000	.999	1.001	1.001	1.000	.998	.994	.993	1.000	.998	.997	.997
4	1.000	1.002	1.006	1.008	1.000	.998	.992	.989	1.000	.999	.997	.996
5	1.000	1.000	1.000	1.001	.999	.993	.974	.963	.999	.996	.985	.979
6	1.000	.998	.994	.992	.997	.976	.928	.907	.998	.988	.963	.951
7	1.000	1.000	1.000	1.001	.997	.979	.930	.902	.999	.990	.965	.952
8	1.000	1.000	1.000	.999	.976	.857	.577	.311	.988	.924	.792	.679
9	1.000	1.001	.999	.995	.967	.853	.674	.475	.982	.913	.820	.761
10	.954	.905	1.029	1.114	.752	.363	.087	.026	.860	.557	.274	.116
11	.998	.985	.962	.955	.990	.925	.783	.717	.995	.962	.887	.851
12	.983	.915	.848	.831	.956	.807	.698	.677	.978	.893	.818	.801
13	.999	.994	.985	.983	.999	.995	.989	.987	1.000	.998	.994	.994
14	.973	.865	.769	.749	.998	.987	.976	.973	.999	.995	.990	.989

Inelastic Scattering Matrix

$\sigma_{in}(i,i+k)$ at k equal to

	0	1	2	3	4	5	6	7	8	9	10
1	.0037	.0670	.2224	.4035	.3370	.2113	.0755	.0227	.0066	.0015	.0003
2	.0387	.2344	.4251	.3551	.2226	.0795	.0239	.0069	.0016	.0003	.0001
3	.1527	.5206	.1194	.1617	.0814	.0280	.0089	.0036	.0009	.0000	.0000
4	.1471	.3937	.1880	.0089	.0030	.0008	.0002	.0001	.0000	.0000	.0000
5	.0000	.0921	.1118	.0574	.0160	.0043	.0011	.0002	.0000	.0000	.0000
6	.0000	.0000	.0000	.0000	.0000	.0000	.0000	.0000	.0000	.0000	
7	.0000	.0000	.0000	.0000	.0000	.0000	.0000	.0000	.0000		
8	.0000	.0000	.0000	.0000	.0000	.0000	.0000	.0000			
9	.0000	.0000	.0000	.0000	.0000	.0000	.0000				
10	.0000	.0000	.0000	.0000	.0000	.0000					
11	.0000	.0000	.0000	.0000	.0000						
12	.0000	.0000	.0000	.0000							
13	.0000	.0000	.0000								
14	.0000	.0000									
15	.0000										

TABLE 2. Group Constants for East Reactor Calculations (^{239}Pu)

Infinite Dilute Cross Sections

Groups	σ_T	σ_F	ν	σ_C	σ_{inel}	σ_{el}	μ_e	ξ	$\sigma_{D(e)}$
1	7.0558	2.2345	3.902	.0000	1.1710	3.6504	.8122	.00169	.0129
2	7.8229	1.8934	3.539	.0000	1.4646	4.4650	.7772	.00193	.0179
3	7.7704	1.9918	3.295	.0000	1.2288	4.5498	.7083	.00249	.0236
4	7.3270	1.9532	3.126	.0027	1.0678	4.3032	.5349	.00394	.0297
5	7.1623	1.7572	3.015	.0447	.8420	4.5184	.4268	.00484	.0384
6	8.2310	1.5855	2.948	.1004	.7246	5.8205	.3620	.00539	.0454
7	9.9819	1.4841	2.909	.1653	.5078	7.8246	.2733	.00513	.0696
8	11.4184	1.5144	2.890	.2086	.3586	9.3368	.1336	.00731	.0989
9	12.4338	1.5166	2.879	.2485	.2643	10.4044	.0563	.00796	.1076
10	13.3191	1.6326	2.874	.5060	.2263	10.9543	.0364	.00813	.1156
11	14.6159	1.9845	2.872	.8583	.1680	11.6051	.0349	.00814	.1228
12	15.8738	2.4738	2.871	1.2484	.0141	12.1375	.0334	.00816	.1286
13	17.7941	3.2752	2.870	1.8923	.0000	12.6266	.0319	.00817	.1339
14	21.2692	5.0019	2.870	3.1867	.0000	13.0806	.0304	.00818	.1390
15	27.7962	8.4947	2.870	5.8028	.0000	13.4987	.0289	.00819	.1437
16	36.0882	13.1127	2.870	8.7711	.0000	14.2044	.0274	.00821	.1514
17	46.2207	20.4083	2.870	12.2526	.0000	13.5598	.0259	.00822	.1447
18	99.1798	54.5426	2.870	27.3287	.0000	17.3085	.0244	.00823	.1850
19	74.2168	24.6454	2.870	35.4798	.0000	14.0916	.0229	.00825	.1509
20	185.5117	105.7331	2.870	65.7859	.0000	13.9927	.0214	.00826	.1501
21	73.6529	33.6720	2.870	27.9456	.0000	12.0353	.0199	.00827	.1292
22	23.7573	9.0037	2.870	3.0242	.0000	11.7294	.0184	.00828	.1261

TABLE 2. (contd)

Self-Shielding Factors

		f_f				f_c				f_t			f_e		
σ_o	T °K	10^3	10^2	10	0	10^3	10^2	10	0	10^2	10	0	10^2	10	0
300	10	1.000	1.000	1.000	1.000	1.000	1.000	1.000	1.000	1.000	1.000	1.000	1.000	1.000	1.000
900	10	1.000	1.000	1.000	1.000	1.000	1.000	1.000	1.000	1.000	1.000	1.000	1.000	1.000	1.000
2100	10	1.000	1.000	1.000	1.000	1.000	1.000	1.000	1.000	1.000	1.000	1.000	1.000	1.000	1.000
	11	1.000	.997	.992	.992	1.000	1.000	1.000	1.000	1.000	.980	.952	.998	.994	.991
	11	1.000	1.000	1.000	1.000	1.000	1.000	1.000	1.000	1.000	1.000	.985	1.000	1.000	1.000
	11	1.000	1.000	1.000	1.000	1.000	1.000	1.000	1.000	1.000	1.000	1.000	1.000	1.000	1.000
	12	.998	.985	.943	.918	.998	.985	.949	.933	.979	.908	.847	.994	.977	.967
	12	1.000	.998	.998	1.000	1.000	1.000	1.000	1.000	.992	.950	.891	.998	.994	.993
	12	1.000	1.000	1.000	1.000	1.000	.000	1.000	1.000	.999	.979	.926	1.000	1.000	1.000
	13	.994	.953	.843	.782	.992	.941	.810	.742	.936	.793	.700	.982	.944	.926
	13	.997	.980	.934	.922	.998	.984	.958	.975	.965	.848	.731	.991	.971	.962
	13	.999	.997	1.005	1.053	1.001	1.007	1.066	1.186	.983	.896	.756	.997	.992	.998
	14	.985	.900	.722	.639	.979	.860	.628	.523	.858	.651	.549	.958	.899	.876
	14	.992	.943	.827	.779	.991	.933	.807	.764	.907	.698	.554	.976	.931	.914
	14	.996	.973	.924	.938	.997	.977	.962	.929	.942	.745	.552	.987	.962	.957
	15	.968	.810	.561	.469	.949	.717	.383	.252	.742	.502	.402	.921	.851	.830
	15	.980	.872	.667	.597	.973	.828	.571	.475	.806	.523	.388	.946	.881	.860
	15	.989	.920	.784	.799	.986	.905	.767	.823	.859	.546	.372	.965	.914	.904
	16	.944	.741	.513	.448	.893	.557	.257	.170	.608	.403	.334	.861	.787	.768
	16	.963	.804	.584	.518	.936	.678	.381	.286	.675	.418	.333	.892	.812	.789
	16	.976	.857	.668	.625	.960	.775	.523	.464	.739	.439	.336	.918	.840	.819
	17	.901	.641	.418	.346	.840	.497	.269	.210	.532	.376	.335	.853	.799	.784
	17	.931	.705	.471	.392	.891	.591	.340	.267	.588	.401	.351	.873	.812	.794
	17	.952	.764	.536	.452	.925	.672	.419	.336	.648	.438	.377	.893	.827	.808
	18	.793	.487	.297	.248	.666	.311	.164	.134	.334	.219	.195	.695	.640	.627
	18	.829	.519	.314	.261	.739	.369	.191	.153	.354	.223	.197	.715	.651	.636
	18	.861	.559	.342	.284	.799	.434	.231	.184	.386	.234	.204	.739	.668	.651
	19	.705	.319	.152	.112	.654	.276	.127	.094	.265	.188	.171	.775	.735	.726
	19	.767	.366	.169	.122	.732	.328	.147	.106	.284	.191	.172	.789	.740	.729
	19	.822	.428	.197	.140	.797	.395	.178	.127	.316	.197	.174	.808	.747	.733
	20	.690	.354	.201	.164	.636	.280	.146	.117	.223	.133	.114	.848	.815	.807
	20	.730	.376	.208	.169	.694	.311	.156	.124	.228	.133	.113	.853	.816	.808
	20	.771	.407	.221	.177	.749	.354	.174	.136	.240	.133	.112	.860	.818	.808
	21	.657	.365	.273	.256	.595	.251	.141	.120	.332	.289	.281	.961	.955	.954
	21	.696	.378	.276	.258	.641	.266	.144	.122	.333	.289	.281	.962	.955	.954
	21	.740	.399	.282	.262	.692	.290	.151	.127	.338	.289	.280	.963	.956	.954
	22	1.000	1.000	1.000	1.000	1.000	1.000	1.000	1.000	1.000	1.000	1.000	1.000	1.000	1.000
	22	1.000	1.000	1.000	1.000	1.000	1.000	1.000	1.000	1.000	1.000	1.000	1.000	1.000	1.000
	22	1.000	1.000	1.000	1.000	1.000	1.000	1.000	1.000	1.000	1.000	1.000	1.000	1.000	1.000

TABLE 2. (contd)

Inelastic Scattering Matrix

$\sigma_{in}(i,i+k)$ at k equal to

	0	1	2	3	4	5	6	7	8	9	10
1	.0002	.0089	.0776	.2850	.3806	.3211	.1375	.0454	.0138	.0032	.0009
2	.0022	.0418	.2399	.4299	.4385	.2111	.0740	.0232	.0054	.0012	.0003
3	.0102	.1292	.3253	.4139	.2280	.0858	.0279	.0067	.0015	.0003	.0001
4	.0422	.2866	.4893	.1626	.0610	.0202	.0045	.0011	.0003	.0000	.0000
5	.3340	.2736	.1569	.0562	.0166	.0036	.0009	.0002	.0000	.0000	.0000
6	.5230	.1599	.0377	.0037	.0003	.0001	.0000	.0000	.0000	.0000	
7	.4072	.0846	.0114	.0037	.0007	.0002	.0000	.0000	.0000		
8	.2777	.0757	.0050	.0001	.0000	.0000	.0000	.0000			
9	.2020	.0578	.0034	.0008	.0002	.0000	.0000				
10	.1360	.0903	.0000	.0000	.0000	.0000					
11	.0478	.0831	.0348	.0023	.0000						
12	.0000	.0000	.0102	.0030							
13	.0000	.0000	.0000								
14	.0000	.0000									
15	.0000										

TABLE 3. Fundamental Mode Calculations for Zebra Assembly 6A

	MC^2	1DX (ETOX) [26 Groups]
k_{eff}	0.9828	0.9838
δk_{eff} for δT^{U238} (1100→300 °K)	0.0084	0.0075
δk_{eff} for $\delta N^{Na} = +0.001$	0.0069	0.0069
$\sigma_f^{U235}/\sigma_f^{Pu239}$	1.0875	1.0796
$\sigma_f^{U238}/\sigma_f^{Pu239}$	0.0399	0.0397
$\sigma_c^{U238}/\sigma_f^{Pu239}$	0.1585	0.1562
$\sigma_c^{Pu239}/\sigma_f^{Pu239}$	0.2128	0.2118
$\sigma_f^{Pu240}/\sigma_f^{Pu239}$	0.2672	0.2673
$\sigma_c^{Pu240}/\sigma_f^{Pu239}$	0.2382	0.2357
$\sigma_c^{B10}/\sigma_f^{Pu239}$	1.4359	1.4186

REFERENCES

1. W. W. Little, Jr., et al. "Numerical Comparison of Data Processing Codes for Fast Reactors," submitted for presentation at the NS&E Seattle meeting June 1969.

2. Group Constants for Nuclear Reactor Calculations, edited by I. I. Bondarenko. Consultants Bureau, New York, 1964.

3. H. C. Honeck. ENDF/B, Specification for an Evaluated Nuclear Data File for Reactor Applications, BNL-50066 (T-46). Brookhaven National Laboratory, Upton, New York. May 1966.

4. W. W. Little, Jr., and R. W. Hardie. FCC-IV, A Revised Version of the FCC Fundamental Mode Fast Reactor Code, BNWL-450. Pacific Northwest Laboratory, Richland, Washington, 1967.

5. R. W. Hardie and W. W. Little, Jr. 1DX, A One-Dimensional Diffusion Code for Generating Effective Nuclear Cross Sections, BNWL-954. Pacific Northwest Laboratory, Richland, Washington, 1969.

6. D. M. O'Shea, B. J. Toppel, and A. L. Rago. MC^2-A Code to Calculate Multigroup Cross Sections, ANL-7318. Argonne National Laboratory, Argonne, Illinois, 1967.

7. W. Romberg. "Vereinfachte Numerische Integration," Det. Kong. Norske Videnskaber Selskab Forhandlinger, Band 28, Nr. 7, 1955.

8. R. N. Hwang. "Doppler Effect Calculations with Interference Corrections," Nucl. Sci. Eng., vol. 21, p. 523. 1965.

9. Handbook of Mathematical Functions, edited by M. Abramowitz and I. A. Stegun, Dover Publications, Inc., 1965. p. 916.

10. F. T. Adler, G. W. Hinman, and L. W. Nordheim. The Quantitative Evaluation of Resonance Integrals, GA-350. General Atomics Division, General Dynamics Corporation, San Diego, California, 1958.

APPENDIX A

RESONANCE SELF-SHIELDING FACTORS - $f^I_{x_j}(\sigma^I_j, T)$

APPENDIX A

RESONANCE SELF-SHIELDING FACTORS - $f^I_{x_j}(\sigma^I_j, T)$

A partial derivation of the expression for the resonance self-shielding factors $f^I_{x_j}(\sigma^I_{o_j}, T)$ will be given in this appendix. For a more detailed derivation and discussion see Bondarenko.[2] The equations and definitions from Section II will be assumed in this appendix.

In the multigroup scheme the neutron balance equations are given as[5]

$$-\frac{1}{3\Sigma^I_{tr}} B^2\phi^I + \frac{\chi^I}{k_{eff}} \sum_{j=1}^{NG} (\nu^j \Sigma^j_f)\phi^j - (\Sigma^I_c + \Sigma^I_f)\phi^I$$

$$+ \sum_{j=1}^{I-1} \Sigma(j\to I)\phi^j - \sum_{j=i+1}^{NG} \Sigma(I\to j)\phi^I = 0, \quad I = 1,2,\ldots,NG, \qquad (A.1)$$

where

$$\phi^I = \int^I \phi(E)dE \qquad (A.2)$$

and

NG = number of energy groups,

B^2 = buckling,

k_{eff} = effective multiplication constant,

χ^I = fission source fraction in group I,

Σ^I_x = macroscopic group average cross sections for transport, fission and capture (x = tr, f, and c),

$\Sigma(I\to j)$ = macroscopic downscattering cross section from group I to j.

The macroscopic group average cross sections for fission, capture, and elastic scattering appear linearly in Equation (A.1) and are given in terms of the following integral expression

$$\Sigma_x^I = \int^I \phi(E)\Sigma_x(E,T)dE/\phi^I \qquad (x = f,c,e). \tag{A.3}$$

The appropriate total macroscopic group average cross section is defined in a reciprocal sense due to its direct relation to the transport cross section[2] and is given as

$$\frac{1}{\Sigma_t^I} \equiv \int^I \frac{\phi(E)dE}{\Sigma_t(E,T)} \Big/ \phi^I. \tag{A.4}$$

The microscopic group average cross sections $\bar{\sigma}_{x_j}^I$ are then defined by the following expression

$$\Sigma_x^I \equiv \sum_{j=1}^{NI} N_j \bar{\sigma}_{x_j}^I \qquad (x = f,c,e,t), \tag{A.5}$$

where N_j is the atom density of the jth isotope and NI is the number of isotopes in the medium. Since the macroscopic cross section is given as

$$\Sigma_x(E,T) = \sum_{j=1}^{NI} N_j \sigma_x(E,T) \qquad (x = f,c,e,t), \tag{A.6}$$

Equation (2.1) of Section II follows from the above equations

$$\bar{\sigma}^{I}_{x_j} = \int^{I} \sigma_{x_j}(E,T)\phi(E)dE \Big/ \int^{I} \phi(E)dE \quad (x = f,c,e). \tag{2.1}$$

From Equation (2.2), Equation (2.1) becomes

$$\bar{\sigma}^{I}_{x_j} = \int^{I} \frac{\phi_o(E)\sigma_{x_j}(E,T)dE}{\Sigma_t(E,T)} \Big/ \int^{I} \frac{\phi_o(E)dE}{\Sigma_t(E,T)} \quad (x = f,c,e). \tag{A.7}$$

In order to simplify Equation (A.7) use is made of the variable σ_{o_j} which is defined by the following equation

$$\Sigma_t(E,T) \equiv N_j\sigma_{t_j}(E,T) + N_j\sigma_{o_j}(E,T). \tag{A.8}$$

With this definition, Equation (A.7) becomes

$$\bar{\sigma}^{I}_{x_j} = \int^{I} \frac{\phi_o(E)\sigma_{x_j}(E,T)dE}{[\sigma_t(E,T) + \sigma_{o_j}(E,T)]} \Big/ \int^{I} \frac{\phi_o(E)dE}{[\sigma_t(E,T) + \sigma_{o_j}(E,T)]}$$

$$(x = f,c,e). \tag{A.9}$$

The reactor composition dependence in $\bar{\sigma}^{I}_{x_j}$ thus arises from the variable $\sigma_{o_j}(E,T)$. In the Bondarenko scheme,[2] $\sigma_{o_j}(E,T)$ in Equation (A.9) is replaced by its "flux-weighted" value averaged over the ith group $[\sigma_{o_j}(E,T) \rightarrow \sigma_{o_j}{}^{I}(T)]$.

In the ETOX code, $\bar{\sigma}^{I}_{x_j}$ cross sections are calculated for a given fixed set of $\sigma^{I}_{o_j}$ values. The $\bar{\sigma}^{I}_{x_j}$ cross section for a given reactor composition can then be obtained by interpolating on this set.

When the above approximation is used, the expression for the total microscopic group average cross section follows from the relation

$$\Sigma_t^I = N_j \bar{\sigma}_{t_j}^I + N_j \sigma_{o_j}^I \tag{A.10}$$

That is,

$$\bar{\sigma}_{t_j}^I = \frac{\int^I \frac{dE}{[\sigma_{t_j}(E,T) + \sigma_{o_j}^I]}}{\int^I \frac{dE}{[\sigma_{t_j}(E,T) + \sigma_{o_j}^I]^2}} - \sigma_{o_j}^I . \tag{A.11}$$

The self-shielding factor equations are now obtained using Equations (A.9), (A.11), (2.4), and (2.5);

$$f_{x_j}^I(T,\sigma_{o_j}^I) = \frac{1}{\langle \sigma_{x_j} \rangle^I} \frac{\left\langle \frac{\sigma_{x_j}}{\sigma_{t_j} + \sigma_{o_j}^I} \right\rangle^I}{\left\langle \frac{1}{\sigma_{t_j} + \sigma_{o_j}^I} \right\rangle^I} \quad (x = f,c,e), \tag{2.6}$$

$$f_{t_j}^I(T,\sigma_{o_j}^I) = \frac{1}{\langle \sigma_{t_j} \rangle^I} \left[\frac{\left\langle \frac{1}{\sigma_{t_j} + \sigma_{o_j}^I} \right\rangle^I}{\left\langle \frac{1}{(\sigma_{t_j} + \sigma_{o_j}^I)^2} \right\rangle^I} - \sigma_{o_j}^I \right]. \tag{A.12}$$

APPENDIX B

RESONANCE REGION FORMULAS

APPENDIX B

RESONANCE REGION FORMULAS

The following expressions give the formulas for the cross sections (barns) calculated in the resonance region for a temperature T(°K) and energy E(ev) in the laboratory system:

$$\sigma_f(E,T) = \sum_{s=1}^{N} \sum_{r=1}^{N_s} \sigma_f^s(E,T)_r + \sigma_{f_F}(E), \tag{B.1}$$

$$\sigma_c(E,T) = \sum_{s=1}^{N} \sum_{r=1}^{N_s} \sigma_c^s(E,T)_r + \sigma_{c_f}(E), \tag{B.2}$$

$$\sigma_e(E,T) = \sum_{s=1}^{N} \sum_{r=1}^{N_s} \sigma_e^s(E,T)_r + \sigma_p(E) + \sigma_{e_f}(E), \tag{B.3}$$

$$\sigma_t(E,T) = \sigma_f(E,T) + \sigma_c(E,T) + \sigma_e(E,T), \tag{B.4}$$

where

$s = (\ell, j)$,

ℓ = orbital angular momentum quantum number,

j = total angular momentum quantum number,

N = the number of s values,

N_s = the number of resonances for a given pair of values of ℓ and j,

$\sigma_{x_f}(E)$ = "floor" correction cross sections (x = f,c,e), (B.5)

$$\sigma_x^s(E,T)_r = 6^s o_r(E) \frac{\Gamma_{x_r}^s}{\Gamma_r^s(E)} \psi(\xi_r^s, X_r^s) \qquad (x = f,c), \tag{B.6}$$

$$\sigma_e^s(E,T)_r = 6^s_{o_r}(E)\left(\frac{\Gamma^s_{e_r}(E)}{\Gamma^s_r(E)}\,\psi(\xi^s_r,X^s_r) + \varphi_\ell(E)\chi(\xi^s_r,X^s_r)\right), \qquad (B.7)$$

$$\sigma_p(E) = \frac{4\pi}{K^2}\sum_\ell (2\ell+1)\sin^2\varphi_\ell(E), \qquad (B.8)$$

$$6^s_{o_r}(E) = \frac{4\pi}{K^2}\,g_j\,\frac{\Gamma^s_{e_r}(E)}{\Gamma^s_r(E)},$$

$$\Gamma^s_r(E) = \Gamma^s_{f_r} + \Gamma^s_{c_r} + \Gamma^s_{e_r}(E),$$

$\varphi_\ell(E)$ = phase shift ($\varphi_o = Ka$, $\varphi_1 = Ka - \tan^{-1}Ka$),

$K = 2.19685 \times 10^{-3}\,(AWR/1 + AWR)\,\sqrt{E}$,

a = channel radius,

AWR = weight ratio of target to that of the neutron,

$g_j = (2j+1)/2(2I+1)$,

I = spin quantum number of the target nucleus,

$\psi(\xi,X)$ = Doppler-broadened line-shape function†

$$= \frac{\xi\sqrt{\pi}}{2}\,\mathrm{REW}\left(\frac{\xi X}{2},\frac{\xi}{2}\right),$$

$\chi(\xi,X)$ = Doppler-broadened line-shape function

$$= \xi\sqrt{\pi}\;I_m W\left(\frac{\xi X}{2},\frac{\xi}{2}\right),$$

W = a complex probability integral (calculated using subroutine QUICKW[6]),

† *Exact definitions and integral properties of the $\psi(\xi,X)$ and $\chi(\xi,X)$ functions are given in Reference 10.*

$$\xi_r^s(E) = \Gamma_r^s(E)/\Delta(E,T),$$

$$\Delta(E,T) = (4EKT/AWR)^{\frac{1}{2}} \quad (K = 8.6167 \times 10^{-5}),$$

$$X_r^s(E) = 2(E-E_r)/\Gamma_r^s(E),$$

Resolved

$$\Gamma_{f_r}^s = \text{constant} = \Gamma_{f_r}^s(E_r),$$

$$\Gamma_{c_r}^s = \text{constant} = \Gamma_{c_r}^s(E_r),$$

$$\Gamma_{e_r}^s(E) = \sqrt{\frac{E}{E_r^s}}\,\Gamma_{e_r}^s(E_r),$$

Unresolved

$\Gamma_{c_s}(E^*)$ = constant = Γ_{c_s},

$\Gamma_{f_s}(E^*)$ = tabulated function (interpolation used to find value at E^*),

$$\Gamma_{e_s}(E^*) = \Gamma_{e_s}^o \sqrt{E^*}\, V_\ell(E^*)\mu_s,$$

$\Gamma_{e_s}^o$ = reduced neutron width,

$V_\ell(E^*)$ = penetration factor: $V_o = 1$, $V_1 = (K_s^*a)^2/[1 + (K_s^*a)^2]$,

$K_s^* = c_s\sqrt{E^*}$ (c_s given with other unresolved parameters in file 2 ENDF/B),

μ_s = number of degrees of freedom in the neutron width distribution.

APPENDIX C

PROGRAM DETAILS FOR THE UNRESOLVED CALCULATIONS

APPENDIX C

PROGRAM DETAILS FOR THE UNRESOLVED CALCULATIONS

The calculations of the J and K integrals and the statistical brackets $\langle \rangle_p$ use the methods given in the MC^2 code.[6]

The J and K integrals are evaluated by breaking the infinite interval into two finite intervals plus a remainder term. In particular, the code assumes

$$J(\beta,\xi) = \int_0^\infty \frac{\psi(\xi,X)}{\psi(\xi,X) + \beta}\, dX = \int_0^{20/\xi} \frac{\psi}{\psi + \beta}\, dX + \int_{20/\xi}^{200/\xi} \frac{\psi}{\psi + \beta}\, dX + REMJ, \tag{C.1}$$

where since

$$\psi(\xi,X) \xrightarrow[\xi X >> 1]{} \frac{1}{1 + X^2}, \tag{C.2}$$

$$REMJ = \int_{200/\xi}^\infty \frac{\psi}{\psi + \beta}\, dX \simeq \frac{1}{\beta} \int_{200/\xi}^\infty \frac{dX}{(a^2 + X^2)} = \frac{1}{\beta a}\left(\frac{\pi}{2} - \tan^{-1}\frac{200}{\xi a}\right), \tag{C.3}$$

$$a = \sqrt{\frac{1 + \beta}{\beta}}\ . \tag{C.4}$$

$$K(\beta,\xi) = \int_0^\infty \frac{\psi(\psi + 2\beta)}{(\psi + \beta)^2}\, dX = J(\beta,\xi) + \int_0^\infty \frac{\beta\psi}{(\psi + \beta)^2}\, dX$$

$$= J(\beta,\xi) + \int_0^{20/\xi} \frac{\beta\psi}{(\psi + \beta)^2}\, dX + \int_{20/\xi}^{200/\xi} \frac{\beta\psi}{(\psi + \beta)^2}\, dX + REMK, \qquad (C.5)$$

where

$$REMK \simeq \frac{1}{2a^2}\left((1 + a^2)\, REMJ - \frac{1}{\beta a}\frac{(1 - a^2)(200/a\xi)}{[(200/a\xi)^2 + 1]}\right). \qquad (C.6)$$

The integrals in the above equations are calculated using 16-point Gaussian gradrature.[9]

The statistical brackets $< >_p$ which are integrations over the Porter-Thomas (chi-squared) distributions use 10-point integration in the neutron-width distribution and 5-point integration in the fission width distributions, both for one or two degrees of freedom. To do this,[6] for a given value of N (N is 5 for fission-width and 10 for neutron-width), the area under the distribution curve is divided into N equal parts such as to determine boundary points X_I

($I = 0, N$; $X_o = 0$; $X_n = \infty$). In other words

$$\int_{X_I^n}^{X_{I+1}^n} P_n(y)dy = \frac{1}{N}\,. \qquad (C.7)$$

Within each interval X_I^n, X_{I+1}^n, then, average values for y are determined, defined as

$$y_{I+1}^n = N \int_{X_I}^{X_{I+1}} yP_n(y)dy. \qquad (C.8)$$

With the above procedure to determine y_I's for the neutron-width distribution and z_I's for the fission-width distribution, the code calculates the statistical brackets by the following double summation:

$$\langle f \rangle_p \equiv \int_0^\infty \int_0^\infty f(y,z)P_n(y)P_m(z)dydz \simeq \frac{1}{50} \sum_{I=1}^{5} \sum_{j=1}^{10} f(y_j^n, z_I^m). \qquad (C.9)$$

Tables C-1 and C-2 list the values of y_i^n and z_i^n used in the code.[6]

TABLE C-1. Values of y_I^n Used for Integration of Neutron-Width Distributions with One or Two Degrees of Freedom.

Index, I	Degrees of Freedom, n	
	1	2
1	0.0052543	0.0517550
2	0.0371740	0.163089
3	0.103133	0.288398
4	0.207850	0.431720
5	0.359875	0.599144
6	0.574320	0.800477
7	0.879486	1.05263
8	1.33502	1.39297
9	2.10558	1.91582
10	4.39230	3.30400

TABLE C-2. Values of z_I^n Used for Integration of Fission-Width Distributions with One or Two Degrees of Freedom.

Index, I	Degrees of Freedom, n	
	1	2
1	0.0212093	0.107400
2	0.155477	0.360070
3	0.467072	0.699863
4	1.10710	1.22312
5	3.24914	2.60955

APPENDIX D

SUBROUTINE DESCRIPTIONS

APPENDIX D

SUBROUTINE DESCRIPTIONS

A brief description of all the subroutines as they appear in the listing will be given in this Appendix.

ETOX	Main program of the code. Calls ZERO, INPUT, PROCES, OUTPUT, OUTPDX.
ZERO	Zeros out arrays in Common.
ERROR	Prints error messages when calculation is beyond limitations of the code.
INPUT	Reads input data.
PROCES	Control link for reading ENDF/B and calculating group constants. Calls ENDFB, AVSEC, RESON, FFACNR, ZERO, INELAS.
ENDFB	Control link for reading ENDF/B. Calls HEADR, LOCISO, FILE1, FILE2, FILE3.
HEADR	Reads ENDF/B ID record.
LOCISO	Locates isotopes on ENDF/B.
FILE1	Reads File 1 which contains $\nu(E)$ information and other general information.
RUSSIN	Generates input data which is same as "Russian" book (Reference 2). Calls FFEL.
FFEL	Generates "Russian" EMAXFF and EMINFF.
FILE2	Reads File 2 which contains resonance parameters.
FILE3	Reads File 3 which contains "smooth cross sections". Calls REMT, SETUP1.
REMT	Locates a particular cross section type, prints if missing or not. Calls CAPSUM, MISS.
CAPSUM	Forms the total capture cross section by summing all capture components. This is done at fine group points.
TERP2	Interpolates a series of points according to ENDF/B specifications.
TERP1	Interpolates a single point according to ENDF/B specifications.
MISS	Prints out missing cross section types in File 3.
WCP	Writes capture cross sections to drum.

SETUP1	Sets up the fine group energy mesh. Calculates fission spectrum at fine group points for E ≥ EG (MGBL2+1). Calls FFLUX.
FFLUX	Generates a fission spectrum shape of flux at a group energy E.
NA23	Calculates resonance cross sections from resonance parameters at fine group points. Used for the isotope Na-23.
AVSEC	Controls calculations of $\langle\nu\rangle$, $\langle\xi\rangle$, $\langle\mu\rangle$ from fine group data. Also $\langle\sigma_f\rangle$, $\langle\sigma_c\rangle$, $\langle\sigma_e\rangle$ if no File 2 information. Calls AVER.
RETREV	Recalls from drum locations the fine group cross sections.
AVER	Calculates infinite dilute cross sections from the fine group cross sections ($\langle\sigma_x\rangle$).
RESON	Control link for resonance region calculations using resonance parameters. Calls AVSECR, RELIB, RRES, URES.
AVSECR	Controls calculation of $\langle\sigma_f\rangle$, $\langle\sigma_c\rangle$, $\langle\sigma_e\rangle$ in the non-resonant region. Calls AVER.
RELIB	Reads tape used in QUICKW calculations.
RRES	Performs and controls resolved calculations. Calls SETUFG, ROMB.
SETUFG	Sets up energy mesh for the ultrafine groups in the resolved region. Determines which resonances contribute to a given ultrafine group. Determines the average "floor" cross sections for each ultrafine group.
ROMB	Calculates resolved resonance integrals over each ultrafine group using the Romberg method.[7] Calls SR.
SR	Generates integrands used in the ROMB calculations. Calls QK.
QK	Calls QUICKW.
QUICKW	Generates ψ and χ line shape functions.
URES	Performs and controls unresolved calculations. Calls SETUPU, AJK.
SETUPU	Sets up energy mesh for the unresolved groups. Interpolates to find fission widths at the boundaries of these groups.
AJK	Calculates J and K integrals (Appendix C).

FFACNR	Calculates self-shielding factors for resonance regions not described by resonance parameters, from the fine group data.
INELAS	Performs and controls inelastic scattering calculations. Calls RETRE1, FILE5, INTERP, INTORP, ERRF.
RETRE1	Reads File 3 for the inelastic or (n,2n) smooth cross sections.
FILE5	Reads File 5 for the inelastic or (n,2n) partial energy distributions.
INTERP	Interpolation scheme used for (n,n') or (n,2n) cross sections.
INTORP	Interpolation scheme used for (n,n') or (n,2n) inelastic probabilities.
ERRF	Calculates the error function.
OUTPDX	Prints and punches data in the 1DX format.
OUTPUT	Prints and punches data in the FCC-IV format.

APPENDIX E

ENERGY BOUNDARIES OF VARIOUS GROUP STRUCTURES AND REGIONS

APPENDIX E

ENERGY BOUNDARIES OF VARIOUS GROUP STRUCTURES AND REGIONS

Figure (E-1) diagrams the energy boundaries of the various group structures and regions for the calculation of a typical isotope,† where:

EG(I) = lower energy bound for the Ith group ($\Delta u \simeq 0.50$, $u = \ln E/E_o$)

EF(I) = lower energy bound for the Ith fine group ($\Delta u \simeq 0.01$)

EUF(I) = lower energy bound for the Ith ultrafine group (unresolved region, $\Delta u \simeq 0.01$)

EURES(I) = lower energy bound for the Ith unresolved group (E^*_I)

EL(1) = lower energy bound resolved region

EL(2) = lower energy bound unresolved region

EMINFF = lower energy bound self-shielded region

EMN1EF = lower energy bound fission flux region

EH(1) = upper energy bound resolved region

EH(2) = upper energy bound unresolved region

EMAXFF = upper energy bound self-shielded region

NG = number of groups

NFGT = number of fine groups

NUF = number of ultrafine groups

NURG = number of unresolved groups

MFFL = lowest group number for self-shielding calculations

MFFU = highest group number for self-shielding calculations

MGBL2+1 = lowest group number using fission spectrum for flux

MRL = lowest group number for resonance calculations

MRU = highest group number for resonance calculations.

---

† *Due to space limitations the number of fine groups per group is shown to be on the order of ten rather than the typical fifty or more.*

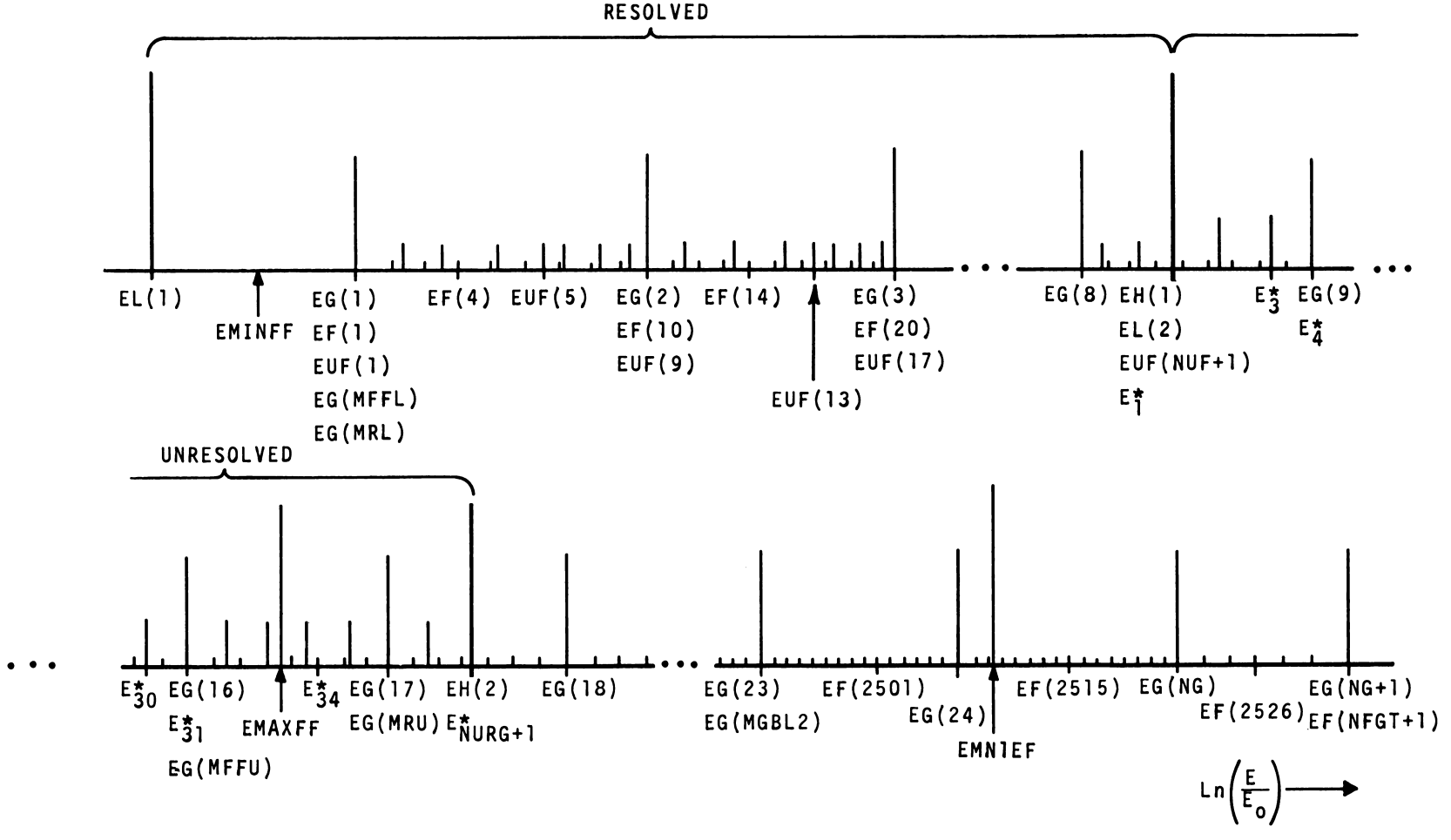

FIGURE E-1. Energy Boundaries of Various Group Structures and Regions.

APPENDIX F

CODE DETAILS AND LIMITATIONS

APPENDIX F

CODE DETAILS AND LIMITATIONS

ETOX reads three tapes (see Figure 2-1), the PCF (program) tape, a table containing the complex probability integral W, and the standard ENDF/B binary data tape. The code requires 65K available fast memory plus 100K words random access drum storage (see Figure 2-1). The code also requires the ability to overlay core storage and presently uses 3 overlays. The program language used is "standard" FORTRAN-IV on a UNIVAC 1108 computer.

Listed below in addition to those specified in ENDF/B are limitations in the present ETOX code:

Maximum number of groups	-	99
Maximum number of fine groups	-	2700
Maximum number of σ_o values	-	6
Maximum number of temperature values	-	5

APPENDIX G

INPUT INSTRUCTIONS

APPENDIX G

INPUT INSTRUCTIONS

Card read input data will be discussed in this appendix.† This data consists of two types called "primary" and "secondary" parameters. The primary input parameters are those that must be read in. They include isotope number and name, ENDF/B ID tape number, group energy structure, sets of temperature and σ_o values, and self-shielding factor energy boundaries. The code includes an option to internally read in the standard "Russian"[2] input which includes all of the primary data except the isotope number, name and ENDF/B ID tape number. The secondary data consists of accuracy parameters which are read internally in the code but can be overridden as an option with the input cards. Their values have been adjusted to give roughly four-place accuracy or better in the group constants with a minimum running time for the code. The following table gives the specific card input instructions:

TABLE G-1. Card Input Instructions.

Variable	Columns	Description
Card 1:	Format (2I5, 1X, A6, 8I5)	(To run a series of isotopes, repeat from this card.)
MAT	1-5	ENDF/B isotope number (see Table G-2).
IDTAP	6-10	ENDF/B tape ID number.
INAME	12-17	Isotope name to be punched on output card.
LNSRI	18-22	If LNSRI=0, then standard "Russian" input will be used. (See Appendix D, subroutine Russian. If this variable is zero, cards 2-6 will be deleted.) If LNSRI≠0, then cards 2-6 are required.

† *Tape input is discussed in Appendix F.*

TABLE G-1. (contd)

Variable	Columns	Description
LNSTI	23-27	If LNSTI=0, then secondary input parameters are internally read in by the code. If LNSTI≠0, then secondary input parameters are read on cards 7 and 8.
LP1	28-32	If LP1=0, then FCC-IV Format will be written and punched. If LP1=1, 1DX Format will be written and punched. If LP1=2, both 1DX, FCC-IV Format will be written and punched.
LN5	33-37	Number of downscattering groups + 1

If LNSRI≠0, then cards 2-6 are required.

Card 2: Format (16I5)

NTEMP	1-5	Number of temperatures at which the self-shielding factors are to be calculated.
NSIGO	6-10	Number of σ_o values.
NG	11-15	Number of groups.

Card 3: Format (6E12.5)

TT(1)	1-12	Temperature (°K) values at which F-Factors are to be calculated.
TT(2)	13-24	
.	.	
.	.	
TT(NTEMP)	.	

Card 4: Format (6E12.5)

SIGO(1)	1-12	σ_o (barns) values.
SIGO(2)	13-24	
.	.	
.	.	
SIGO(NSIGO)	.	

TABLE G-1. (contd)

Variable	Columns	Description
Card 5:	Format (6E12.5)	
EG(1)	1-12	Group boundaries beginning with lowest energy EG(1)(eV).
EG(2)	13-24	
.	.	
.	.	
.	.	
EG(NG+1)	.	
Card 6:	Format (6E12.5)	
EMAXFF	1-12	Maximum energy for F-Factor calculations.
EMINFF	13-24	Minimum energy for F-Factor calculations.

If LNSTI=0, then cards 7-8 are not required.

Card 7:	Format (F12.5, 10I5)	
ANFMPD	1-5	Number of fine-group points per ENDF/B σ_t data points.
NTOL	6-10	Parameter used in resolved calculations.
Card 8:	Format (6E12.5)	
DELMAX	1-12	Maximum lethargy size for fine groups.
EMN1EF	13-24	Minimum energy for non-1/E standard spectrum.
CFF	25-36	Fission spectrum constant.
EPS	37-48	Accuracy parameter Romberg integration.
DELUMX	49-60	Maximum lethargy size for unresolved groups.

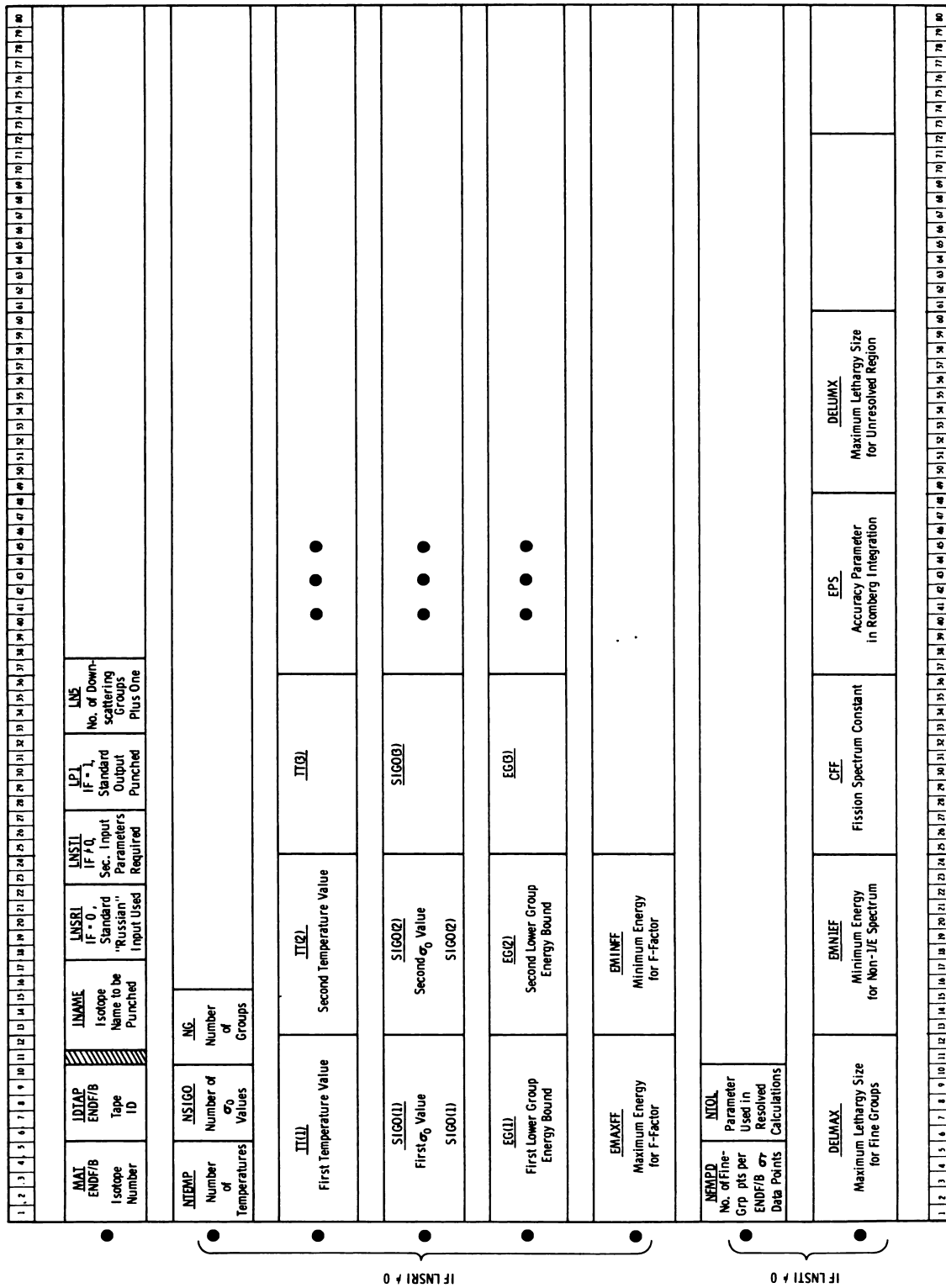

TABLE G-2. ENDF/B Data as Specified by MAT Number.

Material	MAT	Laboratory	Material	MAT	Laboratory	Material	MAT	Laboratory
H-1	1001	BN	Zr-92	1079	BAPL-KAPL	Au-197	1037	BN
H_2O*	1002	GA	Zr-94	1080		Th-232	1038	BN
D-2	1003	BN	Zr-96	1081		Pa-233	1040	BAPL
D_2O*	1004	GA	ZrH*	1023	GA	U-233	1041	GA-ORNL
Li-6	1005	LASL	Nb	1024	GA	U-233 F.P.	1042	BW
Li-7	1006	LASL	Mo	1025	ANL	U-233 F.P.	1066	
Be	1007	GA	Xe-135	1026	BN	U-233 F.P.	1067	
Be-metal*	1064	GA	Sm-149	1027	BN	U-234	1043	GA
BeO*	1008	GA	Eu-151	1028	BN	U-235	1044	KAPL
B-10	1009	ORNL	Eu-153	1029	BN	U-235 F.P.	1045	BW
C	1010	KAPL	Gd	1030	ANL	U-235 F.P.	1068	
Graphite*	1065	GA	Dy-164	1031	BN	U-235 F.P.	1069	
CH_2*	1011	GA	Lu-175	1032	BN	U-236	1046	GA
N-14	1012	ORNL	Lu-176	1033	BN	U-238	1047	BW
O-16	1013	KAPL	Hf-174	1082	BAPL-KAPL	Np-237	1048	ID
Na	1059	APDA	Hf-176	1072		Pu-238	1050	AI
Mg	1014	ANL	Hf-177	1073		Pu-239	1051	GE
Al-27	1015	ORNL	Hf-178	1074		Pu-239 F.P.	1052	BW
Ti	1016	ANL	Hf-179	1075		Pu-239 F.P.	1070	
V	1017	ANL	Hf-180	1076		Pu-239 F.P.	1071	
Cr	1018	WAPD	Ta-181	1035	GE	Pu-240	1053	APDA
Mn-55	1019	BNL	W-182	1060	GE	Pu-241	1054	GA
Fe	1020	WAPD	W-183	1061		Pu-242	1055	AI
Ni	1021	WAPD	W-184	1062		Am-241	1056	ID
Zr-90	1077	BAPL-KAPL	W-186	1063		Am-243	1057	ID
Zr-91	1078					Cm-244	1058	AI

* *Thermal data only.*

DISTRIBUTION

No. of Copies

OFFSITE

1 AEC Chicago Patent Group
G. H. Lee, Chief

38 AEC Division of Reactor Development and Technology
M. Shaw, Director, RDT
Asst Dir for Nuclear Safety
Analysis and Evaluation Br, RDT:NS
Environmental and Sanitary Engrg Br, RDT:NS
Research and Development Br, RDT:NS
Asst Dir for Plant Engrg, RDT
Facilities Br, RDT:PE
Components Br, RDT:PE
Instrumentation and Control Br, RDT:PE
Liquid Metal Systems Br, RDT:PE
Asst Dir for Program Analysis, RDT
Asst Dir for Project Mgmt, RDT
Liquid Metals Projects Br, RDT:PM
FFTF Project Manager, RDT:PM (3)
Asst Dir for Reactor Engrg, RDT
Control Mechanisms Br, RDT:RE
Core Design Br, RDT:RE (2)
Fuel Engineering Br, RDT:RE
Fuel Handling Br, RDT:RE
Reactor Vessels Br, RDT:RE
Asst Dir for Reactor Tech, RDT
Coolant Chemistry Br, RDT:RT
Fuel Recycle Br, RDT:RT
Fuels and Materials Br, RDT:RT
Reactor Physics Br, RDT:RT (3)
W. H. Hannum (3)
P. B. Hemmig (3)
Special Technology Br, RDT:RT
Asst Dir for Engrg Standards, RDT

218 AEC Division of Technical Information Extension

1 AEC Idaho Operations Office
Nuclear Technology Division
C. W. Bills, Director

1 AEC San Francisco Operations Office
Director, Reactor Division

No. of Copies

4 AEC Site Representatives
- Argonne National Laboratory
- Atomics International
- Atomic Power Development Associates
- General Electric Company

7 Argonne National Laboratory
- D. K. Butler
- P. F. Gast
- R. A. Jaross
- LMFBR Program Office
- E. M. Pennington
- N. J. Swanson
- B. J. Toppel

1 Argonne National Laboratory - Idaho Division
- W. G. Davey

2 Atomic Power Development Associates
- Document Librarian
- T. A. Pitterle

10 Atomics International
- H. A. Alter
- D. J. Cockeram (5)
- C. L. Dunford
- Barbara Lemke

Liquid Metal Information Center
- J. J. Droher (2)

4 Babcock & Wilcox Company
Atomic Energy Division
- S. H. Esleeck
- G. B. Garton
- A. Z. Livolsi
- W. A. Wittkopf

5 Bechtel Corporation
- J. J. Teachnor, Project Administrator, FFTF

1 BNW Representative
- N. A. Hill (ZPR III)

8 Brookhaven National Laboratory
- J. Chernick
- Helen Connell
- M. K. Drake
- H. J. C. Kouts
- S. Pearlstein
- A. Prince
- B. R. Sehgal
- T. E. Stephenson

No. of Copies

3 Combustion Engineering
1000 MWe Follow-On Study
R. L. Hellens
L. C. Norderer
W. P. Staker, Project Manager

3 du Pont Company, Aiken
Savannah River Laboratory
D. R. Finch
H. C. Honeck
J. E. Suich

1 General Electric Company, Cincinnati
W. Henderson

7 General Electric Company
Advanced Products Operation
Karl Cohen (3)
P. Greebler
B. A. Hutchins
Bertram Wolfe

Nuclear Systems Programs
D. H. Ahmann

1 General Electric Company, San Jose
Atomic Power Equipment Dept.
P. G. Aline

3 Gulf General Atomic Inc.
General Atomic Division
D. Coburn (2)
D. R. Mathews

3 Idaho Nuclear Corporation
D. R. deBoisblanc
R. A. Grimesey
J. R. Smith

1 Knolls Atomic Power Laboratory
C. R. Lubitz

1 Lawrence Radiation Laboratory, Livermore
R. J. Howerton

3 Los Alamos Scientific Laboratory
M. E. Battat
R. J. LaBauve
R. B. Lazarus

No. of Copies

1 National Bureau of Standards
D. T. Goldman

5 Oak Ridge National Laboratory
C. W. Craven, Jr.
D. J. Dudziak
W. O. Harms
D. C. Irving
S. K. Penny

1 Stanford University
Nuclear Division
Division of Mechanical Engrg
R. Sher

1 United Nuclear Corporation
Research and Engineering Center
R. F. DeAngelis

12 Westinghouse Electric Corporation
Atomic Power Division
Advanced Reactor Systems
R. A. Dannels
J. C. R. Kelly (10)
D. E. Kusner

ONSITE-HANFORD

1 AEC Chicago Patent Group
R. K. Sharp (Richland)

1 AEC RDT Site Representative
P. G. Holsted

4 AEC Richland Operations Office
C. L. Robinson
J. M. Shivley (3)

3 Battelle Memorial Institute

1 Bechtel Corporation
D. H. Weiss (Richland)

1 Westinghouse Electric Corporation
R. Strzelecki (Richland)

No. of Copies

123 Battelle-Northwest

S. O. Arneson
E. R. Astley
Q. L. Baird
J. L. Baker (5)
A. L. Bement, Jr.
R. A. Bennett
K. L. Berrett
D. C. Boyd
C. L. Brown
W. L. Bunch
S. H. Bush
C. P. Cabell
J. J. Cadwell
C. M. Cantrell
J. R. Carrell
J. L. Carter
W. E. Cawley
W. L. Chase
E. D. Clayton
J. C. Cochran
P. D. Cohn
D. L. Condotta
R. R. Cone
G. M. Dalen
F. G. Dawson
B. H. Duane
E. A. Evans
C. L. Fies
L. M. Finch
G. L. Fox
E. E. Garrett
S. M. Gill
V. W. Gustafson
J. W. Hagan
J. P. Hale
J. E. Hanson
R. W. Hardie
R. A. Harris
H. Harty
R. A. Harvey
B. R. Hayward
R. E. Heineman
R. J. Hennig
P. L. Hofmann
B. M. Johnson
H. G. Johnson
E. M. Johnston
R. L. Junkins
R. B. Kidman (5)
D. D. Lanning
R. C. Liikala
C. W. Lindenmeier
W. W. Little
C. E. Love
L. L. Maas
B. Mann
W. B. McDonald
J. S. McMahon
C. A. Munro
C. R. Nash
L. D. O'Dell
A. Padilla
M. G. Patrick
R. D. Peak
R. E. Peterson
O. W. Priebe
W. D. Richmond
W. E. Roake
A. R. Schade
R. E. Schenter (5)
L. C. Schmid
L. E. Schwendiman
F. H. Shadel
J. R. Sheff
D. E. Simpson
R. J. Squires
C. C. Steele
D. D. Stepnewski
D. H. Stewart
K. B. Stewart
C. D. Swanson
J. C. Tobin
K. G. Toyoda
R. C. Walker
A. E. Waltar
J. H. Westsik
J. F. Wett
T. W. Withers
N. G. Wittenbrock
M. R. Wood
J. M. Yatabe
H. S. Zwibel
FFTF Files (10)
Technical Publications (2)
Technical Information (5)
Legal (2)